Circulation Research

ORIGINAL RESEARCH

Cooperative Response to Endocardial Notch Reveals Interaction With Hippo Pathway

Luis Luna-Zurita, Brenda Giselle Flores-Garza, Dimitrios Grivas, Marcos Siguero-Álvarez, José Luis de la Pompa

BACKGROUND: The endocardium is a crucial signaling center for cardiac valve development and maturation. Genetic analysis has identified several human endocardial genes whose inactivation leads to bicuspid aortic valve formation and calcific aortic valve disease, but knowledge is very limited about the role played in valve development and disease by noncoding endocardial regulatory regions and upstream factors.

METHODS: We manipulated Notch signaling in mouse embryonic endocardial cells by short-term and long-term coculture with OP9 stromal cells expressing Notch ligands and inhibition of Notch activity. We examined the transcriptional profile and chromatin accessibility landscape for each condition, integrated transcriptomic, transcription factor occupancy, chromatin accessibility, and proteomic datasets. We generated in vitro and in vivo models with CRISPR-Cas9-edited deletions of various noncoding regulatory elements and validated their regulatory potential.

RESULTS: We identified primary and secondary transcriptional responses to Notch ligands in the mouse embryonic endocardium, and a NOTCH-dependent transcriptional signature in valve development and disease. By defining the changes in the chromatin accessibility landscape and integrating with the landscape in developing mouse endocardium and adult human valves, we identify potential noncoding regulatory elements, validated selected candidates, propose interacting cofactors, and define the timeframe of their regulatory activity. Additionally, we found cooperative transcriptional repression with Hippo pathway by inhibiting nuclear Yap (Yes-associated protein) activity in the endocardium during cardiac valve development.

CONCLUSIONS: Sequential Notch-dependent transcriptional regulation in the embryonic endocardium involves multiple factors. Notch activates certain noncoding elements through these factors and simultaneously suppresses elements that could hinder cardiac valve development and homeostasis. Biorxiv: https://www.biorxiv.org/content/10.1101/2023.03.23.533882v1.full.

GRAPHIC ABSTRACT: A graphic abstract is available for this article.

Key Words: chromatin ■ endocardium ■ epigenomics ■ gene expression profiling ■ heart valves ■ transcription factors

In This Issue, see p 963 | Meet the First Author, see p 965

The endocardium is a specialized endothelium covering the inner surface of the heart.[1] During cardiac development, the embryonic endocardium is a source of cell types and signals essential for the generation of a functional heart.[2] Endocardial Notch signaling is essential for heart development.[3] Delta and Jagged/Serrate ligands expressed on neighboring cells trigger a series of cleavage events in the Notch receptors (Notch1-4) that result in the generation of the Notch intracellular domain (NICD) through γ-secretase activity.[4] NICD translocates to the nucleus, where it binds to a preexisting transcriptional complex including Rbpj (recombination signal binding protein for immunoglobulin kappa J region) to induce target gene expression.[5] In early cardiac development, the endocardium and myocardium are separated by an ECM (extracellular matrix), the cardiac jelly. In the presumptive

Correspondence to: Luis Luna-Zurita, PhD, Intercellular Signalling in Cardiovascular Development & Disease Laboratory, Centro Nacional de Investigaciones Cardiovasculares Carlos III, Melchor Fernández Almagro 3, Madrid 28029, Spain, Email lluna@cnic.es; llunazurita@gmail.com or José Luis de la Pompa, PhD, Intercellular Signalling in Cardiovascular Development & Disease Laboratory, Centro Nacional de Investigaciones Cardiovasculares Carlos III, Melchor Fernández Almagro 3, Madrid 28029, Spain, Email jlpompa@cnic.es

Supplemental Material is available at https://www.ahajournals.org/doi/suppl/10.1161/CIRCRESAHA.123.323474.
For Sources of Funding and Disclosures, see page 1037.

Circulation Research is available at www.ahajournals.org/journal/res

Novelty and Significance

What Is Known?

- The embryonic endocardium is a source of cell types and a crucial signaling center for cardiac valve development and maturation.
- Endocardial Notch signaling directs cellular behaviors for cardiac valve formation, maturation, and adult valve homeostasis.
- NOTCH signaling abrogation is associated with human valve dysmorphology (bicuspid aortic valve) and adult calcific aortic valve disease.

What New Information Does This Article Contribute?

- The existence of a primary transcriptional response after short-term Notch activation that is enhanced after sustained ligand stimulation, and a secondary response triggered after long-term Notch activation.
- The identification of a Notch-dependent transcriptional signature specific for valve development and disease.
- The characterization of the endocardial chromatin accessibility landscape associated with the Notch-dependent transcriptional response, and a set of potential cofactors and the time frame of their activity.
- The identification of a set of noncoding regulatory elements implicated in valve development and homeostasis, and evaluated them in vitro and in vivo.
- The cooperation between the Notch and Hippo pathways through Yap modulation in the endocardium during cardiac valve development.

This research reveals a dual-phase transcriptional response in the endocardium initiated by Notch activation, unveiling a specific Notch-dependent signature for valve development and disease. It defines the chromatin accessibility landscape related to Notch activation and identifies potential cofactors and their activity timelines. Moreover, our study pinpoints critical noncoding regulatory elements affecting valve development, validated through in vitro and in vivo experiments. Notably, this research elucidates the collaboration between Notch and Hippo pathways in the endocardium, emphasizing Yap modulation's significance during cardiac valve development.

Nonstandard Abbreviations and Acronyms

AP-1	activator protein-1
ATAC-Seq	assay for transposase-accessible chromatin with sequencing
BAV	bicuspid aortic valve
CAVD	calcific aortic valve disease
DAR	differentially accessible region
DEG	differentially expressed gene
Dll4	Delta 4
ECM	extracellular matrix
HUVEC	human umbilical vein endothelial cells
MEEC	mouse embryonic endocardial cells
NICD	notch intracellular domain
Yap	yes-associated transcriptional protein

valve territories, this ECM is invaded by mesenchymal cells derived from endocardial-to-mesenchymal transition. The resulting endocardial cushions form the valve primordia and are progressively sculpted through spatiotemporally regulated proliferation and apoptosis of valve interstitial cells and tightly controlled synthesis and ECM organization.[6] Dll4 (Delta 4) binding to Notch1 drives the endocardial-to-mesenchymal transition in the atrioventricular canal and outflow tract regions. Later, remodeling of the valve primordia requires the Jag1 ligand–inducing Notch activity.[7] NOTCH signaling dysregulation is associated with human valvular congenital heart disease and calcific aortic valve disease (CAVD).[8–11]

Much recent effort has focused on discovering noncoding regulatory genomic regions, particularly using genome-wide association studies to identify disease-risk variants, several of which are associated with valve disease.[12–14] These studies highlight the importance of identifying regulatory elements affected by these variants, since the large size of the noncoding genome relative to coding sequences makes it an important mutational target with potential disease-causing consequences. Despite the pivotal role of NOTCH signaling in valve development and disease, the Notch-dependent transcriptional program and regulatory features in the embryonic endocardium remain unknown. Therefore, there is a clear need to identify Notch-activity-dependent regulatory elements, their interacting factors, and the dynamics of their activity.

In this study, we manipulated the Notch signaling pathway in mouse embryonic endocardial cells (MEEC) and identified a complex and sequential transcriptional response with different outputs between short-term and long-term Notch stimulation. Although Jag1 produced a stronger response, there were no ligand-specific effects on the transcriptional output from Jag1 or Dll4. We also examined the dynamics of chromatin accessibility associated with each transcriptional response. By integrating these findings with transcriptional and epigenomic data from developing and adult valves, we identified a Notch-dependent transcriptional signature in valve development and disease. Additionally, we discovered a new set

of noncoding regulatory elements associated with the Notch-dependent transcriptional response and proposed interacting transcription factors. Among these elements, a subset repressed by Notch was active in nonendocardial lineages, suggesting that Notch might suppress their ectopic activity. Further in vitro and in vivo analysis indicated a potential convergence between Notch and Hippo pathways by inhibiting Yap (Yes-associated protein) nuclear translocation during cardiac development.

METHODS

Full methods are provided in the Supplemental Material.

Data are deposited in the NCBI GEO database under accession number GSE223735. RNA-seq from E14.5 WT and *Jag1*$^{flox/flox}$;*Nkx2-5*^{Cre} micro-dissected semilunar valves: GSE74556. RNA-seq from adult control and calcified bicuspid aortic valve (BAV) and tricuspid aortic valve: GSE148219. RNA-seq from human umbilical endothelial cell (HUVEC) transduced with YAPS127A: GSE163459. ATAC-seq from E12.5 mouse endocardial lineage: E-MTAB-3972. ATAC-seq from human mitral valves: PRJNA690001. ATAC-seq from adult mouse cardiomyocytes WT and expressing YAP5SA: GSE123457. ChIP-seq (chromatin immunoprecipitation with sequencing) for RBPJ in HUVEC: GSE85987. ChIP-seq for SMAD in HUVEC: GSE27661. ChIP-seq for SMAD in MDA-MB-231: GSE92443. ChIP-seq for FOXA1, 2, and 3 in MEFs: GSE143444. ChIP-seq for RUNX1 and RUNX2 in MK4: GSE158093. ChIP-seq for GATA4 in mouse endocardium and myocardium at E12.5: GSE156001. ChIP-seq for TEAD4 in in vitro differentiated embryonic stem cells into hemangioblast cells (expressing the receptor tyrosine kinase Flk1): GSE69101. ChIP-seq for TEAD4 in E12/P42 ventricles: GSE124008. A previous version of this work was deposited at BioRxiv (https://www.biorxiv.org/content/10.1101/2023.03.23.533882v1.full).

RESULTS

Jag1 and Dll4 Ligands Differ in Efficiency but Have Similar Gene Targets in MEEC

At E9.5, Notch1 activity is found in the prospective valve endocardium, where both Dll4 and Jag1 ligands are expressed.[7] However, at this stage, only the lack of *Dll4* affects the cellularization of the endocardial cushion tissue (Figure S1A).[7] In contrast, during valve primordium remodeling, Jag1 is the only ligand detected in the valve region. Disruption of endocardial Jag1 signaling results in BAV (Figure S1B).[7]

To define the transcriptional effect of Dll4- and Jag1-induced Notch signaling on the embryonic endocardium, we cultured MEEC[7,15,16] over OP9 (bone marrow-derived mouse stromal cells) expressing Dll4 or Jag1 for 6 or 24 hours. Short-term (6 hours) stimulation with Dll4 yielded 47 differentially expressed genes (DEGs), whereas Jag1 led to 258 DEGs (Figure 1A, top, Table S1). Long-term (24-hour) stimulation increased DEGs for both ligands, with 516 for Dll4 and 1118 for Jag1 (Figure 1A, down). Despite differences in DEG numbers between ligands, the gene expression changes were highly correlated (Figure 1B; Figure S1E), with most DEGs induced by Dll4 also induced by Jag1, differing mainly in the intensity, not the direction of fold changes (Figure 1C; Figure S1C and S1D). Concordantly, Manic Fringe (MFng), which favors Delta-Notch signaling and attenuates Jag/Ser-Notch,[17] was not expressed, suggesting that the differences in transcriptional output between the 2 ligands may reflect this lack of Fng, and that there is no ligand-specific Notch transcriptional response in the endocardium.

Jag1, a known Notch-target gene,[18] was upregulated upon stimulation with both Jag1 and Dll4. Whereas increased Jag1 levels on MEEC membranes could potentially influence cell-autonomous signaling,[19–21] it might also act as an additional stimulus, especially in high-density cultures. Regardless, *Jag1* showed similar upregulation with both ligands (Table S1), enabling a meaningful comparison between their transcriptional responses. These results show that Jag1 is the more effective ligand in terms of signaling output and reveal a lack of ligand-specific target genes in the embryonic endocardium.

Mouse Embryonic Endocardial Cells Initiate a Sequential Transcriptional Response After Notch Ligand Activation

To determine if the detected DEGs resulted directly (as a primary effect) or indirectly from the NICD-Rbpj complex-mediated transcriptional response, we cocultured MEEC over control OP9 for 6 hours with DMSO (vehicle) or the NOTCH-signaling inhibitor RO4929097 (RO; Figure 1F; Table S1). The gene expression changes induced by RO were inversely correlated with those triggered by Dll4 and Jag1 signaling (Figure 1G), confirming the pivotal role of NICD-Rbpj in the observed transcriptional alterations. These RO-induced changes also established a baseline gene expression for comparison with alterations following Dll4 or Jag1 stimulation. Comparison of the transcriptional profiles in the 3 experimental conditions (6 and 24-hour ligand stimulation and RO administration) revealed a 2-phase response to Notch ligand exposure: a primary transcriptional response after NICD nuclear translocation (clusters C1 and C3) that was sustained and intensified over time, and a secondary response (clusters C2 and C4), initiated after prolonged ligand exposure (Figure 1H and 1I; Table S1). In clusters C1 and C3, RO-mediated inhibition of Notch receptor cleavage reduced (C1) or increased (C3) gene expression levels, while expression gradually increased (C1) or declined (C3) during continuous exposure to Notch ligands (Figure 1H and 1I). In contrast, the transcriptional response in clusters C2 and C4 only manifested after 24 hours of ligand exposure (Figure 1H and 1I). Biological function terms overrepresented in a gene ontology

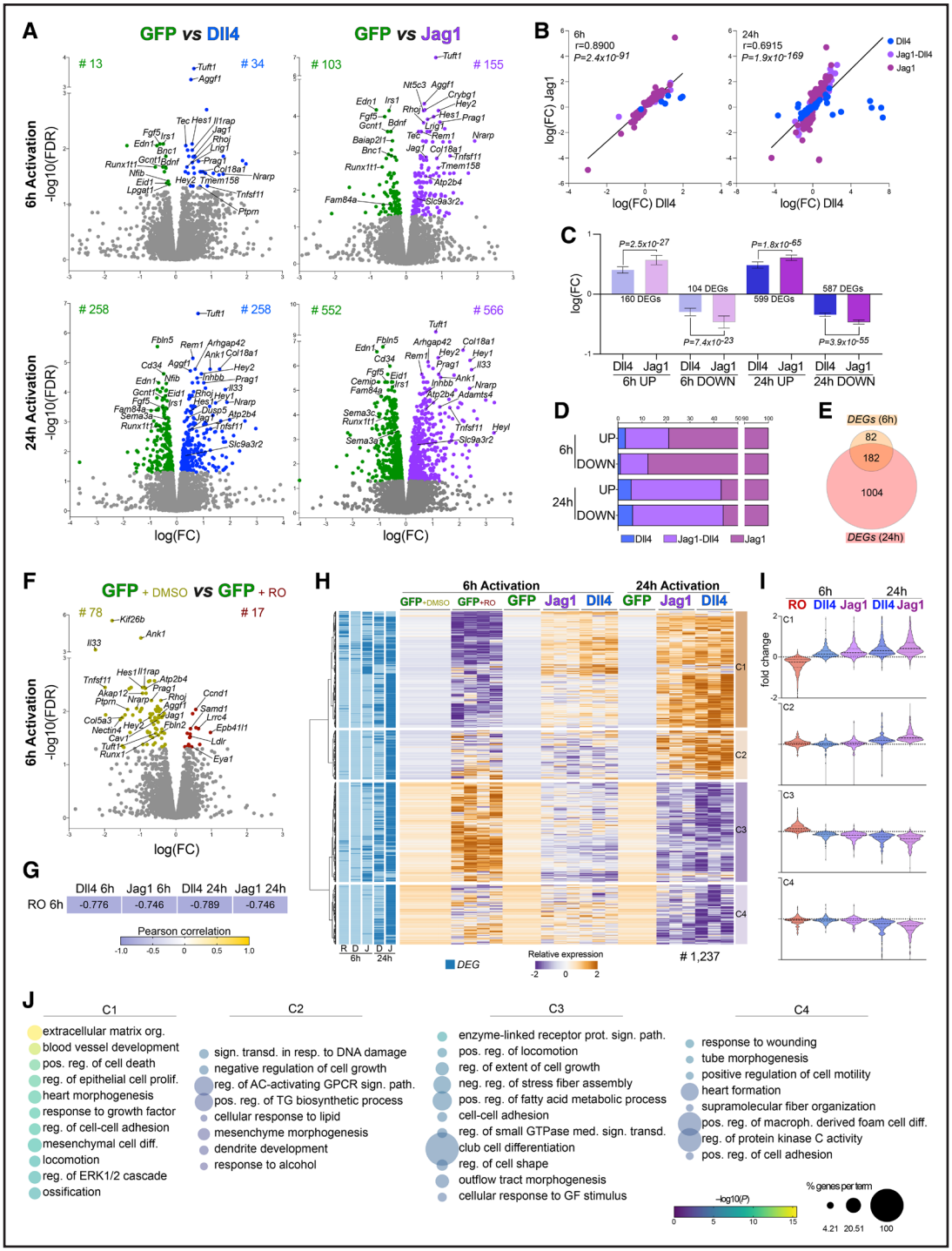

Figure 1. Transcriptional analysis in mouse embryonic endocardial cells after the manipulation of Notch pathway activity.
A, Fold expression changes and associated −log^{10} false discovery rate (FDR) values for each gene detected in mouse embryonic endocardial cells (MEEC) cocultured over OP9-GFP (bone marrow-derived mouse stromal cells expressing green fluorescent protein, control), -Dll4 (Delta 4), or -Jag1 for 6 (top) or 24 hours (bottom). Color indicates upregulation with Dll4 (blue), Jag1 (purple), and downregulation (green). Three biological replicates for each experimental condition. **B**, Fold expression changes after coculture with OP9-Dll4 vs OP9-Jag1 for each differentially expressed gene (DEG) detected after 6 (left) or 24 hours (right). Pearson correlation coefficient. **C**, Mean fold changes in DEGs upregulated and downregulated after Dll4 and Jag1 stimulation for 6 and 24 hours. Wilcoxon matched-pairs signed-rank test. Error bars, 95% CI. Number of genes is represented. **D**, Percentage of DEGs dependent on Jag1 and Dll4 after 6- or 24-hour stimulation. **E**, Proportion of DEGs detected after 6- or 24-hour stimulation. **F**, Fold expression changes and associated −log^{10}(FDR) values for each gene detected in MEEC cocultured with OP9-GFP+DMSO/RO4929097 (RO) for 6 hours. Color indicates upregulation (red) and downregulation (green) with RO. Four biological replicates for each experimental condition. **G**, In DEGs detected in **F**, Pearson correlation between changes in gene expression due to RO, Dll4, or Jag1 activity for 6 or 24 hours. **H**, Hierarchical clustering of DEGs detected in MEEC after RO treatment or cocultured with OP9-Dll4 and -Jag1. **I**, Fold expression changes of DEGs from each cluster. **J**, Enriched gene ontology (biological function) terms for each cluster. The size of the nodes represents the percentage of genes associated with the term. The color code represents the −log^{10}(*P* value) for the enrichment.

analysis of the primary transcriptional response (C1, C3) included extracellular matrix, cell-cell adhesion, locomotion, stress fiber assembly, regulation of the ERK1 (extracellular signal-regulated kinase 1) and ERK2 cascades, and GTPase-mediated signal transduction (Figure 1J; Table S1). C2 genes were primarily associated with transcriptional activity and metabolism, whereas overrepresented function terms in C4 included response to wounding, tube morphogenesis, cell motility, and macrophage differentiation (Figure 1J; Table S1). These findings highlight a complex and sequentially coordinated transcriptional response to Notch ligands.

A Notch-Dependent Gene Signature Associated With Cardiac Valve Development and Disease

To determine if the transcriptional responses observed in MEEC also occur in vivo, we examined 2 available transcriptional datasets. First, we used transcriptional data from microdissected semilunar valves of E14.5 WT and *Jag1*^{flox}*;Nkx2-5*^{Cre} mice, characterized by hyperplastic and dysmorphic valves and a high rate of BAV.[7] Highly expressed genes in WT valves were enriched in C1 and C2 DEGs (Notch-activated DEGs). Conversely, *Jag1*^{flox}*;Nkx2-5*^{Cre} valves displayed overexpression of C3 and C4 DEGs (Notch-repressed DEGs, Figure 2A, left). These findings confirm that the Notch-dependent transcriptional response observed in vitro recapitulates the natural process occurring in developing semilunar valves. Another recent transcriptional analysis identified an immune-metabolic gene expression signature in human adult calcified bicuspid valves and tricuspid valves.[22] Aortic-valve calcification is the most common form of valvular heart disease and is suppressed by NOTCH activity. Consistently, analysis of this dataset showed that C1 and especially C2 DEGs were significantly more abundant in control valves, indicating downregulation of these genes in CAVD (Figure 2A, right). In contrast, Notch-repressed DEGs showed no significant difference between samples (Figure 2A, right). This finding suggests that transcriptional changes associated with CAVD involve the repression of genes positively regulated by Notch activity in the endocardium.

Given the prevalence of clusters C1 and C2 (positive primary and secondary transcriptional responses) in control conditions in both these models, we investigated their specific role in each context. Hierarchical clustering of gene expression changes showed specifically downregulation in human calcified aortic valves (A1), in developing mouse valves lacking Jag1 signaling (A2), and in both settings (A3; Figure 2B). Gene ontology analysis highlighted the involvement of endothelial, ECM, and ERK signaling-related genes in cluster A2 (downregulated in *Jag1*^{flox}*;Nkx2.5*^{Cre} semilunar valves; Figure 2C), similar to the functions associated with cluster C1 (Figure 1J). Cluster A1 (human calcified valves) was associated with metabolic and proliferative functions (Figure 2C), similar to cluster C2 (Figure 1J). Consistently, C1 DEGs were overrepresented in cluster A2, whereas C2 DEGs were more represented in cluster A1 (Figure 2D), suggesting that the secondary transcriptional response to Notch activity plays an important role in preventing aortic valve calcification. Despite differences, a predicted protein-protein interaction network constructed from A1-3 DEGs revealed significant interactivity within each cluster and among all 3, indicating close association and shared functions among the genes detected in vivo (Figure 2E). Further assessment of the effect Jag1-Notch1 signaling blockade in developing mouse aortic valves identified reduced expression of A1 (*Akap12*), A2 (*Ctgf*), and A3 (*Tgfb2 [transforming growth factor beta-2]* and *Slit2*) genes (Figure 2F). Together, these results confirm the relevance of our in vitro dataset to the study of valve development and disease.

Endocardial Secretion of Notch-Dependent Soluble Proteins

Endocardial Notch signaling involves the expression and secretion of soluble factors that modify adjacent ECM and signal to nearby myocardium.[23] We previously described the Notch-dependent endocardial secretome after stimulation of MEEC with recombinant Notch ligands.[16] Here, we performed RNA-seq on MEEC stimulated with recombinant ligands (see Methods), finding a good correlation with the transcriptional changes identified in the MEEC–OP9 (MEEC over OP9) coculture assay (Figure S2A; Table S3). This consistency allowed us to integrate our transcriptional dataset with the Notch-dependent secretome, identifying gene sets whose endocardial expression and protein secretion change upon Notch manipulation in the same way (clusters II and IV) or in the opposite way (clusters I and III; Figure S2B; Table S3). Integration of these analyses with the in vivo data described in Figure 2A, revealed proteins like Tgfβ2, Fbln2, Col6a1, and Timp3 whose secretion and expression in valve endocardium are affected by Notch disruption during valve development in mice (Figure S2C; Table S3) and in human CAVD (Figure S2D; Table S3). These findings underscore the significance of our dataset in unraveling the role of Notch signaling in valvulogenesis.

Notch-Pathway Manipulation in MEEC Alters Chromatin Accessibility

To identify the regulatory features orchestrating the Notch-dependent transcriptional cascade in the endocardium, we used ATAC-seq to study changes in chromatin accessibility in MEEC after OP9 coculture (OP9-Dll4 and OP9-Jag1 for 6 and 24 hours and OP9+RO for 6 hours). Applying relaxed selection criteria (see Methods), we defined 4229 differentially accessible regions (DARs), 1477 after 6-hour stimulation, 2689 after 24 hours, and 1087 after RO treatment (Figure 3A and 3B; Table S4). Notably, only a few

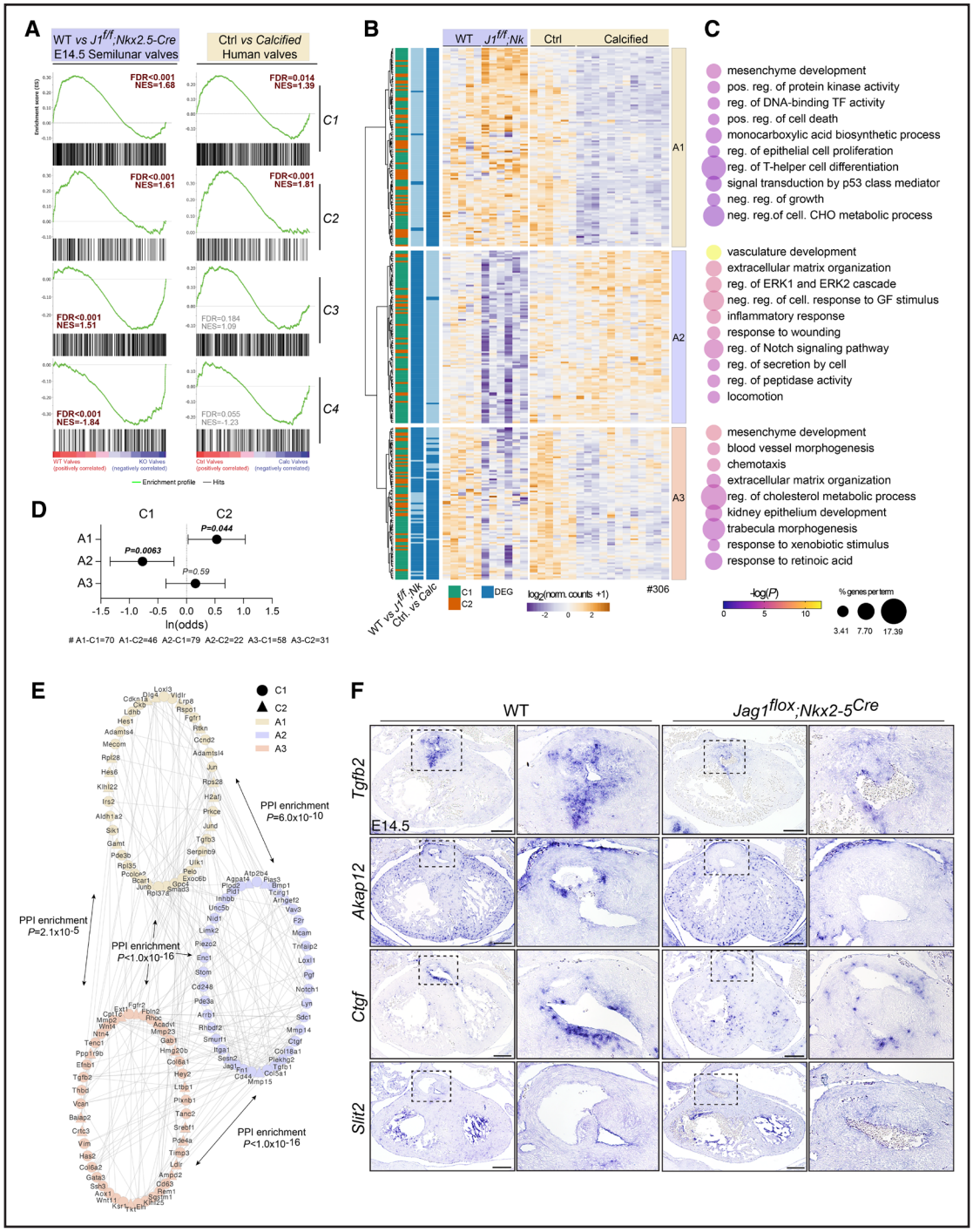

Figure 2. The Notch-dependent transcriptional response in mouse embryonic endocardial cells operates in mouse valve development and human valve disease.

A, Gene-set enrichment analysis showing the distribution of differentially expressed genes (DEGs) located in clusters C1 to C4 from Figure 1H within the ranking of all genes identified in E14.5 WT and *Jag1*^{flox};*Nkx2.5*^{Cre} semilunar valves (left), and in control (Ctrl) and calcified adult human valves (right). False discovery rate (FDR) values represent the statistical significance of the enrichment score. **B**, Hierarchical clustering of cluster C1 and C2 genes significantly enriched in E14.5 WT vs *Jag1*^{flox};*Nkx2.5*^{Cre} semilunar valves or in Ctrl vs calcified human valves. **C**, Enriched gene ontology (biological function) terms for each cluster. The size of the nodes represents the percentage of genes associated with the term. The color code represents the –log^{10}(*P* value) for the enrichment. **D**, Odds ratios and 95% CI for finding C1, C2, or C3 DEGs in clusters A1, A2, or A3. Fisher exact test. Number of genes for each category is indicated. **E**, Protein-protein interactome prediction for genes identified in clusters A1, A2, or A3. The number of predicted interactions between clusters was statistically significant. **F**, In situ hybridization (ISH) analysis of *Tgfb2*, *Akap12*, *Ctgf*, and *Slit2* expression in heart sections from E14.5 WT and *Jag1*^{flox};*Nkx2.5*^{Cre} embryos. Magnified views of the aortic valve are shown to the right. Representative images of 3 experiments. Scale bars: 100 µm. NES indicates normalized enrichment score.

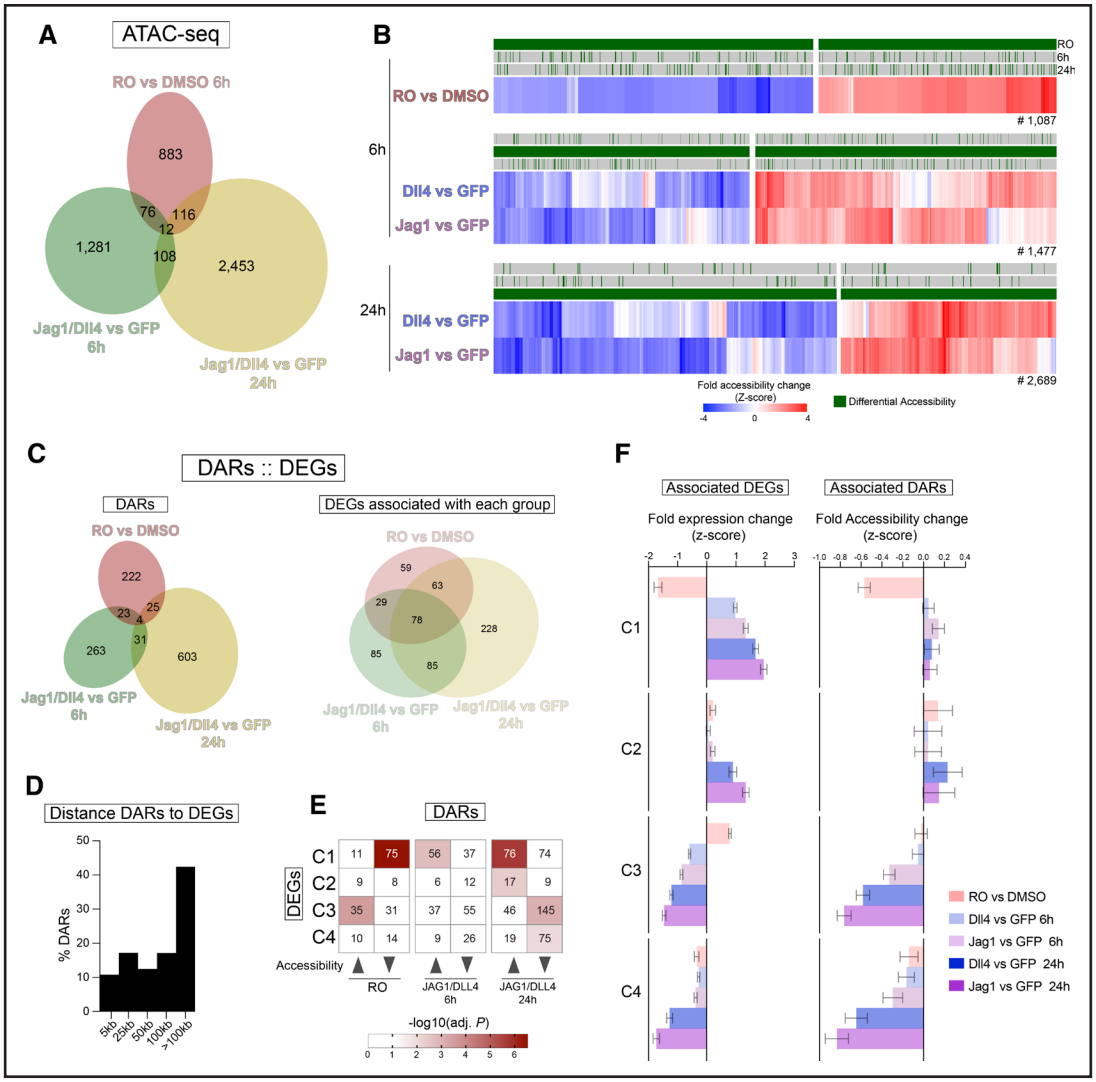

Figure 3. Chromatin accessibility changes and association with gene expression in mouse embryonic endocardial cells after the manipulation of Notch pathway activity.

A, **Left**, Overlap between differentially accessible regions (DARs) detected after RO4929097 (RO) treatment for 6 hours and Notch-ligand stimulation for 6 and 24 hours. Four biological replicates for each experimental condition. **B**, Hierarchical clustering of DARs in each experimental condition. **C**, For DAR-differentially expressed genes (DEG) pairs, overlap between DARs detected in each condition (left) and between DEGs associated to DARs detected at each condition (right). **D**, Distance of DARs from the transcription start sites of the associated DEG. **E**, Enrichment of chromatin accessibility patterns in the regulatory domains of DEGs from each expression cluster. Number of DAR-DEG pairs in each category is represented. Red indicates the significant adjusted *P* value. **F**, **Left**, Median fold expression change in each experimental condition in DEGs from each expression cluster (C1–C4) associated with any DAR. **Right**, Median fold accessibility change (*z*-score) in each experimental condition in DARs associated with DEGs from each expression cluster. Error bars, SEM.

DARs were observed in more than 1 experimental condition (Figure 3A) while gene expression changes were consistently affected by Notch inhibition and activation (Figure 1G; Figure S1C). This specificity was well illustrated when we clustered the 4229 DARs according to their accessibility changes (Figure S3A), showing each cluster (a-g) a major accessibility change exclusively in 1 experimental condition (Figure S3A). For example, clusters b and e were characterized by a strong alteration after RO treatment, with no clear pattern after 6 or 24 hours of ligand exposure. To assess the relevance of each chromatin accessibility profile to the Notch-dependent transcriptional response, we defined a regulatory domain for each DEG (using GREAT, see Methods) and identified the overlapping DARs (defining 1250 DAR–DEG pairs; Table S4). Contrasting the limited overlap among DARs between conditions (Figure 3C, left), DEGs in these pairs were frequently associated with more than 1 DAR from different experimental conditions (Figure 3C, right). Consistent with DARs genome-wide distribution, with 81.7% detected in intergenic or intragenic regions (Figure S3C), 90% of DARs were located farther than 5 kb from the transcription start sites of their associated DEG (Figure 3D). Despite the distal location, changes in accessibility and gene expression in DAR-DEG pairs showed a good

correlation (Figure S3C), supporting a potential regulatory role of the DARs over their paired DEGs.

To identify specific accessibility changes associated with expression changes of the putative DEGs, we assessed the representation of each accessibility pattern within the regulatory domains of each expression cluster (Figure 3E). Consistent with the C1 DEGs expression pattern (Figures 1H and 3F, left), repression by RO and activation after ligand stimulation were the most represented accessibility patterns in the associated DARs (Figure 3E and 3F, right). Concordantly, for cluster C2 (late positive response to ligand activation; Figures 1H and 3F, left), the only enriched pattern in DARs was increased accessibility after long-term ligand stimulation (Figure 3E and 3F, right). These results suggest that the induction and maintenance of C1 DEGs expression require the sequential participation of distinct genomic elements, whereas C2 DEGs seem to depend on regions responding to long-term ligand activity.

Similarly, the early and late transcriptional repression in clusters C3 and C4 (Figures 1H and 3F, left) was reflected in a general repression of accessibility in the associated DARs after Notch ligand stimulation (Figure 3E and 3F). Interestingly, for the response to RO, consistent changes between DARs and the associated DEGs were only evident for cluster C1, indicating that the activity of the NICD-Rbpj complex is confined to this cluster. Together, these results suggest complex and well-coordinated transcriptional regulation in response to Notch ligand signaling.

Multiple Transcription Factors Contribute to the Notch-Dependent Endocardial Transcriptional Response

To identify factors interacting with DARs and potentially orchestrating the observed transcriptional changes, we conducted a known-motif enrichment analysis (see Methods) in DARs from each accessibility pattern (Figure 4A; Table S4). RO-dependent accessibility repression was characterized by RBPJ-binding motifs (Figure 4A), suggesting that the NICD-Rbpj interacting regulatory elements inducing the expression of direct Notch target genes likely reside in these DARs. Supporting this prediction, chromatin accessibility in DARs interacting with RBPJ in HUVEC[24] was inhibited after RO exposure and increased after ligand activation (Figure 4B). Similarly, SMAD (suppressor of mothers against decapentaplegic) binding motifs were overrepresented in DARs repressed by RO (Figure 4A), and DARs interacting with SMAD were repressed after RO treatment, and gradually activated after Notch ligand stimulation[25,26] (Figure 4B). Although crosstalk between Notch and the Smad-dependent Tgfβ/Bmp (transforming growth factor beta/bone morphogenetic protein) pathway has been reported,[27] our analysis suggests that while the presence of potential Rbpj-binding sites in DARs effectively indicates RO-driven accessibility repression, the presence of potential Smad sites alone does not (Figure 4C, left, Figure 4D). A similar pattern was observed for DEGs associated with DARs containing potential binding sites for Rbpj, Smad or both (Figure 4C, right, Figure 4D). These observations suggest that in the endocardium, the downstream effectors of the Tgfß/Bmp pathway primarily interact with genomic regulatory elements recognized by the Notch effector Rbpj (Figure 4C).

For the positive response to Notch-ligand stimulation, motifs recognized by AP-1 (activator protein-1) family members were overrepresented after 6 hours (Figure 4A), and Runx (runt-related transcription factor) and Fox (forkhead box) factors emerged as the strongest candidate mediators of the long-term response (Figure 4A). As predicted by the motif enrichment analysis, DARs interacting with these transcription factors[28,29] displayed increased accessibility following long-term Notch ligand stimulation (Figure 4B).

Notch-activated DARs exhibited a strong correlation with C1 DEGs (Figure 3E and 3F). Accordingly, RBPJ, SMAD, AP-1, and FOX-binding motifs were the most enriched motifs in DARs associated with cluster C1 (Figure 4G; Table S4). Moreover, consistent with the association of DARs activated exclusively after long-term Notch ligand stimulation with C2 DEGs (Figure 3E and 3F), RUNX-binding motifs were the most represented associated with cluster C2 (Figure 4G).

Motif enrichment analysis of DARs showing RO-dependent increased accessibility suggested that Notch pathway activation represses Gata transcription factors activity in the endocardium (Figure 4A). Although this observation is consistent with transcriptional repression of Gata factors by the Notch targets Hes and Hey,[30,31] Gata transcription factors have an active role in the embryonic endocardium[32] and similarly to Notch, their inactivation has been associated with aortic valve disease.[12,33,34] In particular, both Gata4 and Gata6 were downregulated (with statistical significance only for Gata6) by endocardial Notch activity. The integration of Gata4 genome-wide occupancy in embryonic Tie2+ (endocardium) and TnT+ (myocardium) cardiac cells[32] revealed that DARs exclusively occupied by Gata4 in the myocardium are mostly repressed by Notch (Figure 4B, red square). This observation suggests that Notch may restrict Gata activity to the appropriate genomic elements in the embryonic endocardium.

Reduced accessibility after Notch ligand stimulation revealed motifs recognized by the Hippo pathway member Tead (TEA domain transcription factor) (Figure 4A; Table S4). This enrichment was especially prominent after long-term stimulation. Similarly to Gata, the association between Notch-dependent repression and Tead occupancy[35,36] appeared restricted to DARs recognized by Tead exclusively in the myocardium (Figure 4B, red square), suggesting a repressive role of Notch over endocardial Tead activity in these elements. Similarly, motifs recognized by

ORIGINAL RESEARCH

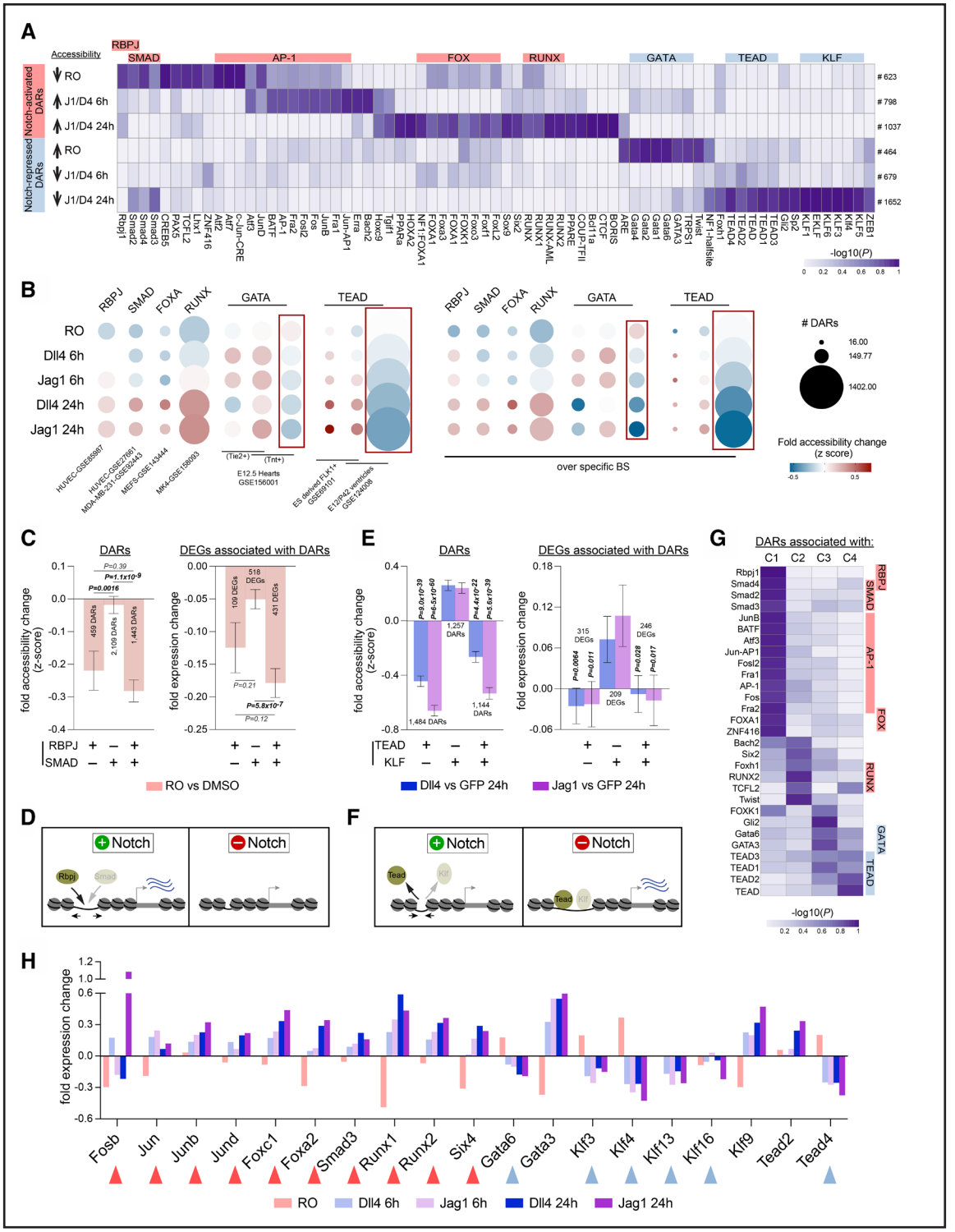

Figure 4. Potential transcription factors controlling gene expression changes in mouse embryonic endocardial cells in response to Notch pathway manipulation.

A, Heatmap showing the −log10(pvalue) of known binding site motifs detected in at least one of the clusters from Figure 3B. **B**, **Right**, Median fold accessibility change (*z*-score) in each experimental condition in differentially accessible regions (DARs) recognized by each transcription factor. **Left**, Similar representation but restricted to DARs presenting specific binding motifs for the assayed transcription factor. The size of the nodes represents the numbers of DARs interacting with each factor. The color code represents average fold accessibility change (*z*-score) in each condition for each group of DARs. **C**, **Left**, Median fold accessibility change (*z*-score) after RO treatment in DARs containing motifs for RBPJ (recombination signal binding protein For immunoglobulin kappa J), SMAD (suppressor of mothers against decapentaplegic), or both. **Right**, Median fold expression changes after RO treatment in differentially expressed genes (DEGs) associated with DARs containing motifs for RBPJ, SMAD, or both. **D**, Proposed Notch-induced Rbpj occupancy in genomic elements repressed by RO treatment. **E**, **Left**, Median fold accessibility change (*z*-score) after 24-hour stimulation with Dll4 (Delta 4)/Jag1 in DARs containing motifs for TEAD (TEA domain transcription (*Continued*)

KLF (Krüppel-like factors) were associated with accessibility repression after long-term Notch-ligand stimulation (Figure 4A) but only when they appeared together with TEAD motifs (Figure 4E, left, Figure 4F). A repressive crosstalk has been reported between Notch and Klf4.[37,38] If Tead activity is involved in this interaction should be further investigated. The implication of the Hippo pathway in controlling Notch-repressed DEGs is supported by the overall downregulation of DEGs associated with DARs containing TEAD motifs, whether or not KLF motifs are present in the same genomic element (Figure 4E, right, Figure 4F). Moreover, TEAD, along with GATA, was the most represented binding motif in DARs associated with C3 and C4 DEGs (Figure 4G).

Transcription factors recognizing the overrepresented motifs exhibited differential expression, often aligning with the chromatin alterations affecting their potential target genomic elements (Figure 4H). This suggests a complex and interdependent regulatory network downstream of NICD. In summary, our findings not only identify a group of noncoding genomic elements that may govern Notch-induced gene expression changes but also highlight various cofactors and temporal dynamics for their roles as transcriptional regulators.

Notch-Dependent Chromatin Accessibility Changes in Embryonic and Adult Cardiac Valves Endocardium

To evaluate the relevance of the MEEC chromatin accessibility profiles in valve development and homeostasis, we compared our data with ATAC-seq data from E12.5 mouse endocardium[39] and human adult mitral valves[14] (Figure 5A; Table S4). Despite the association between NOTCH and aortic valve disease, Notch loss-of-function in developing valves affects both aortic and atrioventricular valves similarly,[7] supporting the use of data from human mitral valves in our study. Fifty-four percentage of MEEC DARs overlapped with accessible regions detected in at least one of these in vivo datasets. Interestingly, the percentage increased to 71% when considering Notch-activated DARs (clusters a-c) and decreased to 41% when considering Notch-repressed DARs (clusters d-g, Figure 5B; Table S4). Furthermore, Notch-activated DARs (a-c) were significantly associated with Notch-induced DEGs (C1-C2) exclusively when these DARs were detected in vivo (Figure 5C). Conversely, Notch-repressed DARs (d-g) were overrepresented near Notch-repressed DEGs (C3-C4) only when these DARs were not detected in vivo (Figure 5C). Together, these results strongly support a role for endocardial Notch as an activator of noncoding regulatory elements essential for valve development and homeostasis while acting as a repressor of elements capable of inducing undesired gene expression.

The integration of both in vitro and in vivo data also enabled us to identify cofactors with a potential role in valve endocardium. For example, in contrast to FOX, RUNX-binding motifs were specifically enriched in Notch-activated DARs and undetected in the in vivo datasets (Figure 5D). This suggests that the coordinated activity of Notch and Runx in the endocardium is not involved in valve development. Conversely, KLF motifs were specifically overrepresented in Notch-repressed DARs, especially when they were also repressed in valves (Figure 5D). This suggests that repression of Klf transcription factors, alongside Tead, in the endocardium may be necessary for valve development and homeostasis.

Next, we generated a list of high-confidence Notch-activated DARs detected in vivo and associated with endocardial Notch target genes in the in vivo data (Figure 5E; Table S4). These selected elements were validated for their capacity to activate potential target genes by using CRISPR-Cas9 gene editing technology in transfected MEEC (Figure S4A; Table S6). Although deletion of each genomic element occurred in only a fraction of the transfected cells (Figure S4B), it significantly reduced the expression of the putative target genes (Figure 5F). This was observed for genomic elements associated with genes downregulated in calcified human valves (*Rara*, *Smad3*, *Akap12*, *Fads3*), in *Jag1*^{flox}*;Nkx2.5-Cre* E14.5 semilunar valves (*Notch1*, *Slc9a3r2*), and in both models (*Timp3*, *Has2*, *Tgfb2*, *Hey2*, *Vcan*). The *Hey2*-associated genomic element *3220* showed high sequence conservation as well as conserved proximity to *Hey2* across species (Figure 5G). To validate its functionality, we generated a knock-out zebrafish model for the *3220* element (Figure 5G and 5H; Table S6). The offspring of the Δ3220 line showed pericardial distension, an unlooped heart, and a bent tail at 96 hours post-fertilization (hpf), mirroring the phenotype of *hey2* loss-of-function models[40–42] (Figure 5G). Consequently, our in vitro and in vivo validation experiments confirm the functional significance of the identified regions.

Notch and Hippo Signaling Pathways Converge in the Endocardium During Heart Valve Development

The integration of MEEC transcriptomic and epigenomic data after Notch manipulation revealed a strong association between gene expression inhibition and repression

Figure 4 Continued. factor), KLF (Krüppel-like factors), or both. **Right**, Median fold expression changes after 24-hour stimulation with Dll4/Jag1 in DEGs associated with DARs containing motifs for TEAD, KLF, or both. **C** and **E**, Mann-Whitney *U* test. Error bars, SEM. Number of DARs and DEGs is indicated. **F**, Proposed notch-induced Tead occupancy in genomic elements repressed by long-term Notch-ligand activity. **G**, Heatmap showing the −log10(pvalue) of known binding motifs detected in **A** and overrepresented in DARs associated with DEGs in each expression cluster (C1–C4). **H**, Fold expression changes of differentially expressed transcription factors whose motif appeared in **A**.

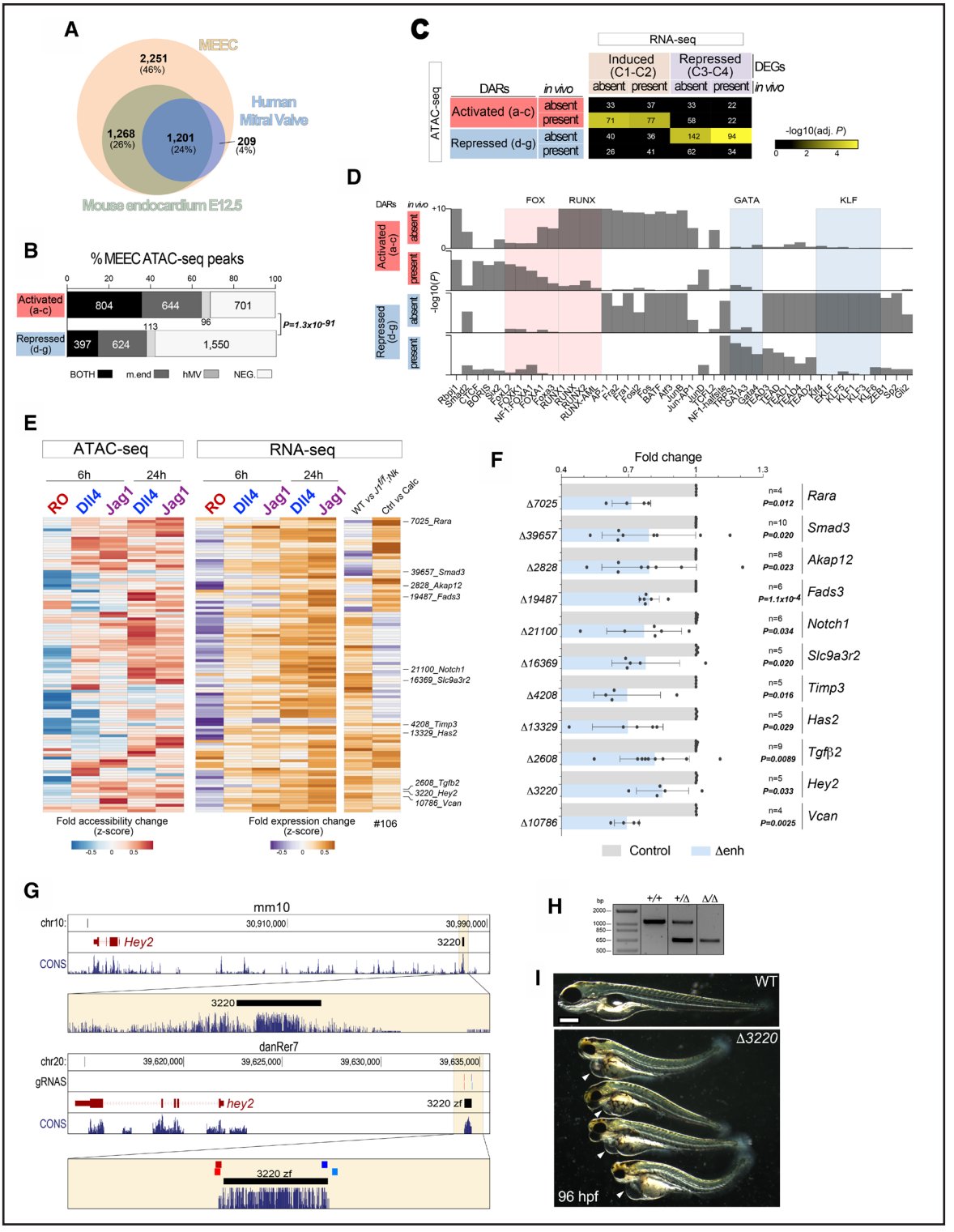

Figure 5. The regulatory potential of Notch-dependent noncoding regulatory elements in mouse embryonic endocardial cells is observed in valve endocardium.

A, Overlap of differentially accessible regions (DARs) detected in mouse embryonic endocardial cells (MEEC) with accessible regions identified in the E12.5 mouse endocardium or in adult human mitral valves. **B**, Proportion of Notch-activated (clusters a-c) and Notch-repressed DARs (clusters d-g) overlapping with accessible regions detected in vivo. χ^2 test. Number of DARs in each category is represented. **C**, Enrichment of DARs from clusters a-c and d-g associated to differentially expressed genes (DEGs) from clusters C1-C2 or C3-C4. DARs and DEGs are stratified according to their presence or absence in vivo. Number of DAR-DEG pairs in each category is represented. Yellow indicates the significant adjusted *P* value. **D**, Statistical representation of binding motifs detected in Figure 4A in DARs from clusters a-c and clusters d-g present or absent in vivo. Bars represent the −log10(*P* value). **E**, DAR-DEG pairs present in vivo and responding positively to Notch activity (clusters a-c and C1 and C2). Heatmaps represent fold accessibility changes in DARs (**left**) and fold expression changes in the (*Continued*)

of genomic elements potentially recognized by Tead transcription factors. Although Tead factors can operate independently of Yap,[43–45] the Hippo pathway downstream effector Yap acts as the Tead main cofactor. To assay the potential interaction between Notch and Yap in the endocardium, we incorporated ATAC-seq data from mouse hearts expressing the transcriptionally active form Yap^{5SA} in the myocardium (a tissue where Notch is inactive)[46] into our endocardial epigenomic dataset. In the myocardium, Yap activation increases the accessibility of Notch-repressed DARs (Figure 6A, top), suggesting a repressive role of Notch in endocardial Yap activity. Notably, most Notch-repressed DARs were absent in in vivo datasets (E12.5 mouse endocardium and adult human mitral valve; Figure 5B), indicating that Notch acts as a repressor of these genomic elements in vivo. Concordantly, the positive response to myocardial Yap in Notch-repressed DARs was more evident in DARs absent in vivo (Figure 6A, top). Furthermore, the highest positive response to Yap was found in Notch-repressed DARs containing TEAD-binding motifs, regardless of their activity in vivo (Figure 6A, bottom). Together, these findings suggest that the negative association between chromatin accessibility and potential Tead-binding sites in MEEC DARs is mediated by Notch-dependent repression of endocardial Yap activity.

To assess the transcriptional consequences of this potential repression, we integrated transcriptional data from HUVEC transduced with the transcriptionally active form Yap^{S127A} [47] to our MEEC–OP9 dataset (clusters C1–C4, Table S5). While a mild antagonism was observed between the transcriptional responses to Yap and Notch in each MEEC cluster (Figure 6B, left), a clear opposite expression pattern emerged when we focused on genes differentially expressed in both MEEC and HUVEC (Notch- and Yap-dependent genes, Figure 6B, right). Two significant enrichments were found: (1) genes repressed by Yap in the Notch-activated transcriptomic clusters C1 and C2 and (2) genes activated by Yap in the Notch-repressed transcriptomic clusters C3 and C4 (Figure 6C). This behavior was mirrored in the mouse in vivo data, where the set of Notch-repressed genes in E14.5 semilunar valves was significantly enriched in genes activated by Yap, and the set of Notch-activated genes was enriched in genes repressed by Yap (Figure 6D; Table S5). Hierarchical clustering of Notch- and Yap-dependent genes, based on their expression changes in vitro and in vivo, revealed the overrepresentation of DEGs with opposite responses to Yap and Notch, both in vitro and in vivo (clusters D and H, Figure 6E and 6F). These DEGs showed a strong association with valve and aortic diseases (GDA score <0.1, DisGeNET database), compared with DEGs where this response was only observed in vitro (clusters B and F, Figure S5A and S5B; Table S5). This emphasized the importance of the cooperation between the Notch and Hippo pathways in valve development.

Gene ontology analysis revealed an enrichment of cytoskeletal and cell junction–related terms highly associated with genes activated by Yap and repressed by Notch, in vivo and in vitro (cluster D, Figure 6G; Table S5). Consistent with cluster D DEGs, the predominant chromatin accessibility pattern in associated DARs was repression by Notch in vivo and in vitro, with a positive response to Yap (Figure 6H). Furthermore, this association showed the highest representation of TEAD-binding motifs (Figure 6I, 71%). Overall, this comprehensive analysis revealed a robust correlation between the epigenomic and transcriptomic Notch-dependent repression of genomic elements and genes that are positively regulated by Yap.

Our findings indicate that endocardial Notch represses Yap-dependent noncoding elements, resulting in the inhibition of direct target genes. We hypothesized that this repression might coincide with a reduction in nuclear Yap content. Exposure to recombinant Jag1 significantly reduced nuclear Yap content in MEEC, whereas exposure to RO increased it (Figure 7A and 7B). This observation aligned with Yap localization predominantly in the cytoplasm in the E9.5 mouse WT endocardium. Conversely, in homozygous mutant embryos with abrogated endocardial Notch activity (*Dll4^{flox};Tie2^{Cre}*), Yap was detected in both cytoplasm and nucleus of valve and ventricular endocardial cells (Figure 7C and 7D). Furthermore, Yap nuclear localization in the *Dll4^{flox};Tie2^{Cre}* myocardium appeared unaltered, supporting that Notch activity exerts a cell-autonomous effect on Yap in endocardial cells. In summary, our results highlight the convergence of Hippo and Notch signaling and suggest that Notch acts as a modulator of Yap activity in the embryonic endocardium (Figure 7E).

DISCUSSION

In this study, we stimulated MEEC with Jag1 and Dll4 ligands expressed on OP9 cells to identify the transcriptomic and epigenomic consequences of Notch manipulation. Our transcriptional analysis defines a primary (short-term) and a secondary (long-term) response to

Figure 5 Continued. associated DEGs (center) in MEEC upon Notch manipulation, and fold expression changes in DEGs in E14.5 WT vs *Jag1^{flox};Nkx2.5^{Cre}* semilunar valves, and in control vs calcified adult human valves (**right**). ID of DARs and associated DEGs tested in **F** are indicated. **F**, qRT-PCR analysis of the candidate target genes in MEEC transfected with the empty vector (control) or with the vector containing the gRNAs specific for each DAR. Four to 10 independent experiments were performed for each gene. Paired *t* test, except for *Smad3* and *Akap12* (Wilcoxon matched-pairs signed-rank test). Error bars, SD. **G**, Location of the Notch-dependent regulatory element (3220) associated with *Hey2* in the mouse and zebrafish genome. Location of gRNAs for zebrafish is indicated. **H**, PCR of genomic DNA from 3 96 hpf zebrafish siblings (wild type, Δ3220 heterozygote, and Δ3220 homozygote). **I**, Bright-field images of 1 sibling control and 4 Δ3220 null embryos at 96 hpf (most represented phenotype in 7 litters, 20 to 30 embryos examined per litter). Arrowheads indicate the pericardial edema. Scale bar, 250 μm.

ORIGINAL RESEARCH

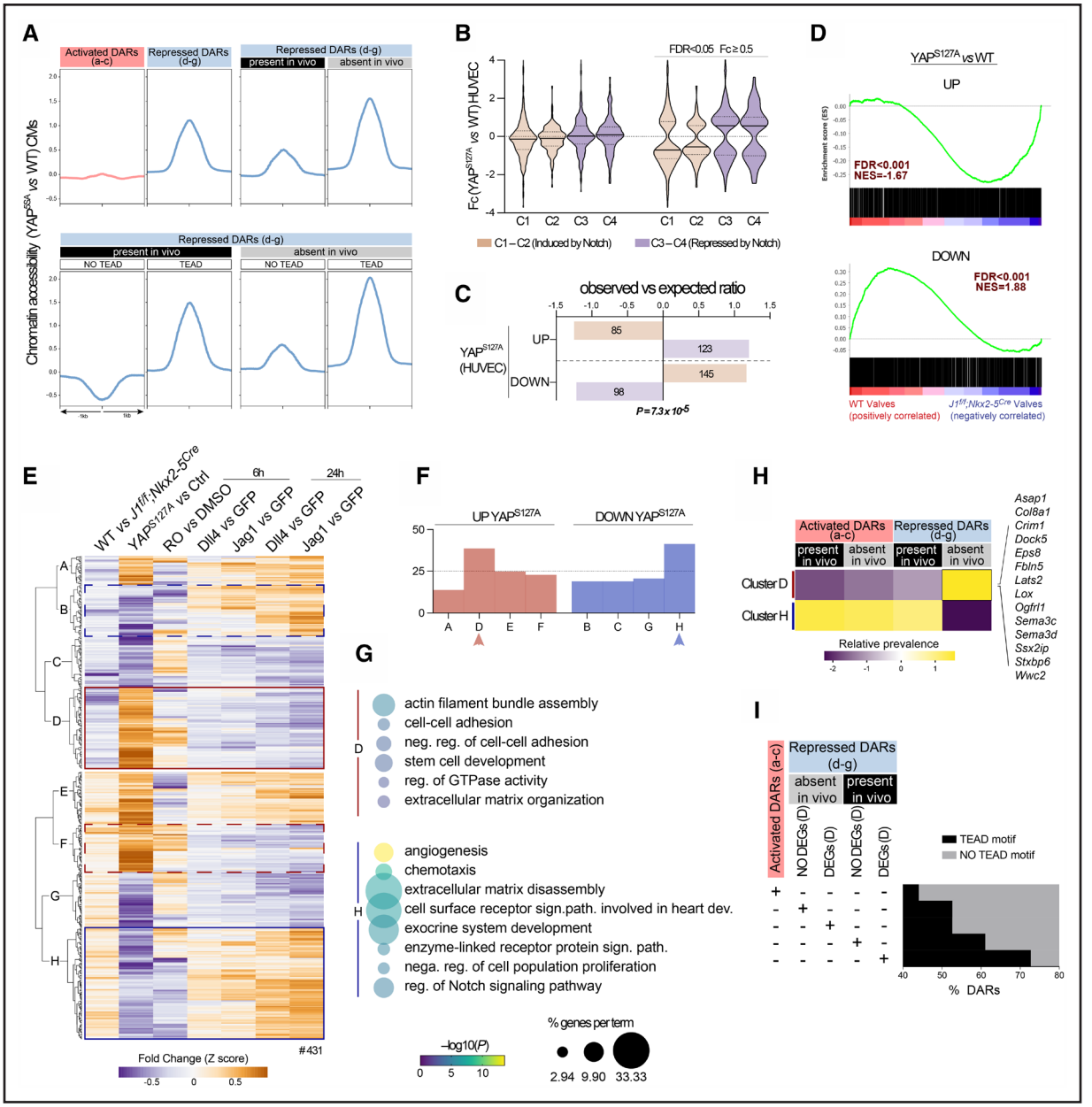

Figure 6. The Hippo and Notch signaling pathways converge in mouse embryonic endocardial cells.
A, In differentially accessible regions (DARs) detected in mouse embryonic endocardial cells (MEEC), differences in chromatin accessibility in mouse cardiomyocytes expressing Yap^{5SA}. Signal was plotted 1 kb upstream/downstream of DARs center. **B**, **Left**, In MEEC transcriptomic cluster (C1-C4), fold expression changes after Yap^{S127A} transduction in human umbilical vein endothelial cells (HUVEC). **Right**, Only MEEC differentially expressed genes (DEGs) differentially expressed in HUVEC are represented. **C**, Statistical enrichment in clusters C1 and C2 or C3 and C4 of genes upregulated or downregulated in HUVEC after Yap^{S127A} transduction. Fisher exact test. Number of genes in each category is indicated. **D**, Gene-set enrichment analysis showing the distribution of Yap^{S127A} -positive (top) and -negative (down) target genes in HUVEC within the ranking of all genes identified in E14.5 WT and *Jag1^{flox};Nkx2.5^{Cre}* semilunar valves. False discovery rate (FDR) values represent the statistical significance of the enrichment score. **E**, Hierarchical clustering of MEEC and HUVEC DEGs detected in E14.5 WT and *Jag1^{flox};Nkx2.5^{Cre}* semilunar valves. Clusters with opposite response to Yap and Notch observed in vitro and in vivo are indicated with a solid line. Clusters with opposite response to Yap and Notch observed only in vitro are indicated with a dashed line. **F**, Percentage of genes from each cluster upregulated or downregulated after Yap^{S127A} transduction in HUVEC. Opposite response to Yap and Notch in vitro and in vivo is the most represented expression pattern in each group (clusters D and H, arrowheads). **G**, Enriched gene ontology (biological function) terms for clusters D and H. The size of the nodes represents the percentage of genes in the cluster associated with the term. The color code represents the $-\log^{10}$(*P* value) for the enrichment. **H**, Relative prevalence of chromatin accessibility patterns in the regulatory domains of DEGs from cluster D and H. **I**, Proportion of DARs containing TEAD-binding motifs under different conditions, such as activation or repression by Notch activity, overlap or no overlap with accessible genomic regions detected in the developing mouse endocardium or adult human valves, or association with DEGs from cluster D. NES indicates normalized enrichment score.

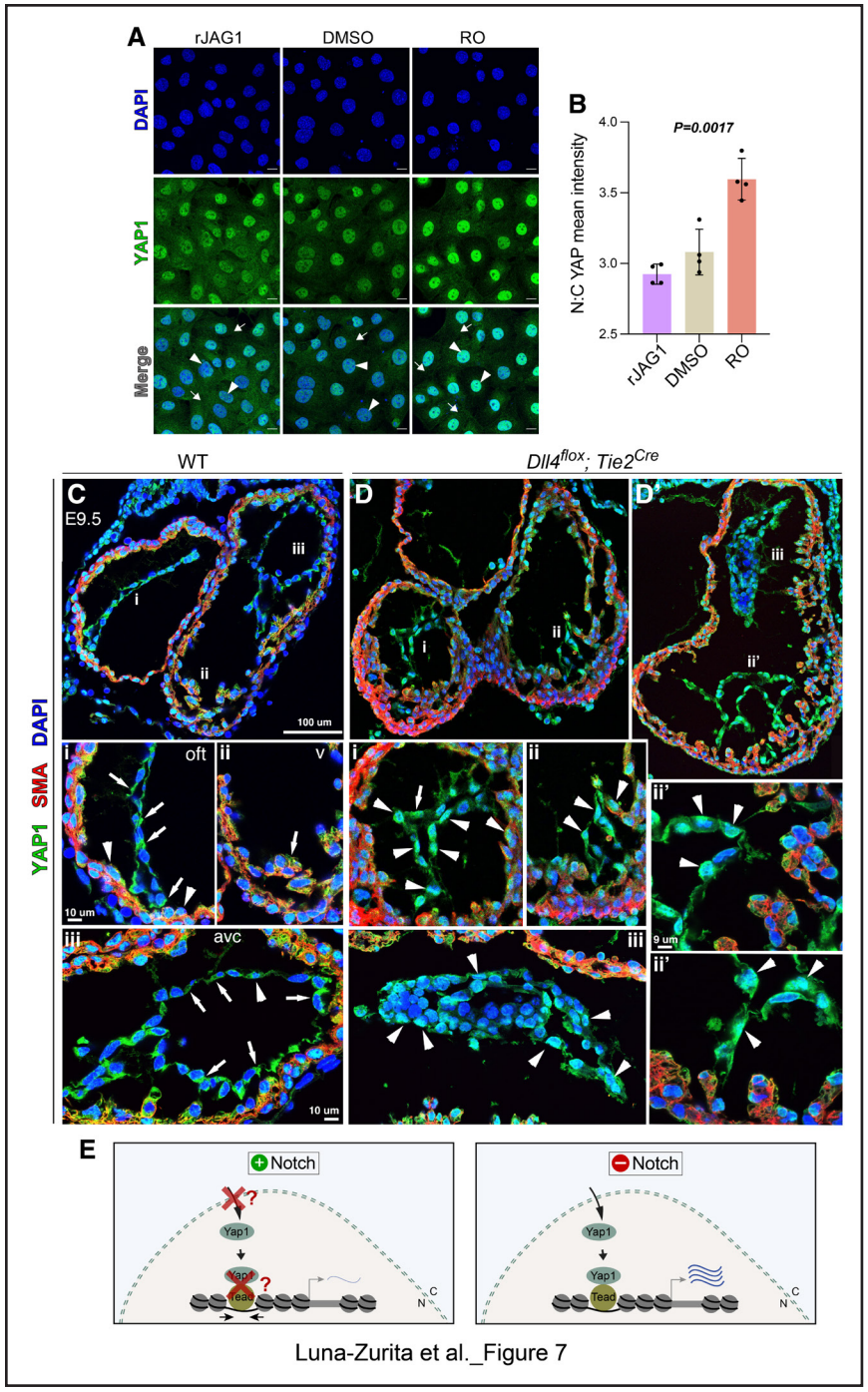

Figure 7. Notch-pathway activity reduces nuclear-Yap1 (yes-associated transcriptional protein 1) in mouse embryonic endocardial cells.
A, Immunofluorescence of Yap1 in mouse embryonic endocardial cells (MEEC) exposed to DMSO, RO, or recombinant JAG1. Nuclei are counterstained with DAPI. Representative images of 4 experiments. **B**, Quantification of the nuclear:cytoplasmic intensity ratio of Yap1. One-way ANOVA. Four experiments (140–301 cells measured per condition and experiment). Error bars, SD. **C** and **D**, E9.5 wild type (**C**) and *Dll4*$^{flox/flox}$;*Tie2*^{Cre} (**D**) transverse heart sections immunostained for Yap1 and α-sma (myocardium), and counterstained with DAPI. General views and insets of outflow tract (**i**), ventricles (**ii, ii'**), and atrioventricular canal (**iii**). Arrowheads point to Yap1 nuclear staining, arrows to Yap1 cytoplasmic staining. Representative images of 3 experiments (2 WT and 2 *Dll4*$^{flox/flox}$;*Tie2*^{Cre} embryos per experiment). Scale bars: 100 µm (**C**, **D**, and **D'**), 10 µm (**i**, **ii**, and **iii**), 9 µm (**ii'**). **E**, Proposed interaction between Notch and Yap1 in the endocardium. Left, wild type (Notch+) endocardium. Our data suggest that Notch prevents Yap1 nuclear translocation, activity of genomic regulatory elements, and/or target gene expression. Right, Notch-deficient endocardium. Nuclear Yap1 is enabled to drive target gene expression ectopically.

Notch signaling activation. The incorporation of in vivo transcriptomic data from developing valves of wild type and Notch mutant mice and from control and diseased adult human valves confirmed the relevance of our findings. Our epigenomic analysis defined a set of Notch-responsive noncoding genomic elements. Despite our permissive criteria to define DARs (see Methods), the subsequent analyses supported our approach: (1) we observed a significant correlation between changes in DARs and associated DEGs; (2) consistency between the DARs response to Notch manipulation and their binding motif composition (ie, RBPJ in DARs repressed by RO activity); (3) significant correlation between the positive response of DARs to Notch activity and accessibility in mouse embryonic endocardium and adult human valves. Together with the validation of the regulatory potential of selected identified genomic elements against the in vitro and in vivo data, the combination of our transcriptional and epigenomic data identified a set of candidate genomic regulatory elements and associated transcription factors that likely operate within a well-defined time frame.

Several genes have been proposed to be Notch-dependent in the endocardium during cardiogenesis, the position of these genes in the Notch-dependent

transcriptional landscape and the cofactors required for their endocardial expression remain unclear. Our transcriptional analysis has revealed 2 distinct phases of this transcriptional response in the embryonic endocardium. The early primary response is triggered by the baseline activity of Notch ligands and gradually increases with ligand stimulation for 6 and 24 hours. Together with RBPJ, SMAD-binding motifs were the most represented motifs in genomic regions repressed by RO. Smad activity is crucial in the atrioventricular canal and outflow tract endocardium to initiate endocardial-to-mesenchymal transition and is induced by Tgfβ2 (endocardium and myocardium) and Bmp2 (myocardium) signaling.[48,49] In the MEEC–OP9 coculture assay, with no signaling from the myocardium, Notch-pathway activation induced *Smad3* and *Tgfb2* expression (and Tgfβ2 secretion) through the activity of at least one specific genomic regulatory element. The presence of RBPJ-binding motifs in most of these potential Smad-dependent regulatory elements suggests a crucial role for Notch not only as a Tgfβ2 activator but also as a necessary cofactor in the transcriptional induction of target genes. Further studies will be needed to determine if myocardial Tgfβ/Bmp signaling to the endocardium operates through Notch-independent genomic elements.

Genomic regions with increased chromatin accessibility after short-term stimulation were enriched in sequences recognized by AP-1, a transcription factor heterodimer composed of proteins from the c-Fos, c-Jun, activating transcription factor (ATF), and JDP (Jun dimerization protein) families and proposed to act in conjunction with Notch.[50,51] The early positive response to Notch-pathway manipulation of *Jun* and *Fosb* (both in cluster C1) suggests these proteins as Notch partners in the transcriptional response of the embryonic endocardium. Similarly, *Foxc1*, expressed in the endocardium and required for outflow tract morphogenesis[52] may recognize the abundant FOX-binding motifs in genomic regions induced by long-term Notch-ligand stimulation. Overall, the association of Notch-responsive genomic elements containing these motifs with C1 DEGs, indicated a sequential activity of specific transcription factors acting cooperatively in response to Notch-pathway activation.

Mutations in NOTCH1 increased the risk of BAV and aortic valve calcification.[10,53,54] This justifies our selection of in vivo datasets to provide biological context for the Notch-dependent transcriptional changes in MEEC. We use a mouse model with disrupted cardiac Notch signaling that develops BAV, as well as adult valves from both healthy individuals and patients with CAVD. Both datasets showed evidence of the primary and secondary positive transcriptional responses to Notch signaling. Downregulation of Notch-responsive endocardial genes in *Jag1*^{flox}*;Nkx2-5*^{Cre} semilunar valves (mostly short-term responsive genes), along with the associated genomic elements identified in mouse endocardium and human valves, allowed us to propose a set of genes and genomic elements potentially involved in semilunar valve development. In contrast to the mouse model, human samples were not selected based on Notch dysregulation. Nevertheless, many of the genes responding positively to Notch (especially after long-term stimulation) were downregulated in CAVD samples. Potential Runx-dependent genomic elements were overrepresented near genes exhibiting a long-term positive response to Notch activity (C2), although these elements were mostly inaccessible in mouse and human valves. *Runx2* derepression has been suggested to induce CAVD in Notch1 haploinsufficient mice,[10] but our MEEC-OP9 coculture system confirmed that Notch actually induces *Runx2*. Similarly, *Runx1*, a Notch target gene in hematopoiesis[55,56] also involved in bone formation,[57] showed a positive response to Notch activation in our dataset. The Notch-dependent transcriptomic signature in CAVD proposed here is associated with metabolic activity and transcriptional regulation, which could be related to a slowed-down metabolic status in calcified valves. In line with our observation, a more complex pro-osteogenic and inflammatory program was proposed to be repressed by Notch endothelial activity.[58] Rather than acting solely as a repressor of calcification,[10] we suggest that Notch, through its interaction with other pathways, regulates a more complex program to maintain valve homeostasis.

Besides the positive transcriptional response, Notch activity also repressed a set of distal genomic elements in the MEEC-OP9 coculture system. Most of these elements were repressed in the developing mouse endocardium and human mitral valves, which aligns with the proposed role of Notch in valve development and homeostasis. TEAD-binding motifs appeared overrepresented in these, indicating an association with genes downregulated by Notch activity. Tead transcription factors require cofactors like the Hippo signaling pathway effectors Yap and Taz.[59] When unphosphorylated, Yap enters the nucleus and interacts with Tead to drive gene expression. Cardiac Yap activity is involved in regulating cardiomyocyte proliferation[60,61] and cytoskeleton remodeling.[62]

Our results identify Notch as a pathway cooperating with Hippo during cardiac development (Figure 7E). Beyond repressing genomic elements potentially recognized by Yap, Notch activation also inhibits many endothelial Yap targets in the embryonic endothelium, both in vitro and in vivo. Furthermore, in vitro and in vivo disruption of endocardial Notch signaling leads to an increase in nuclear Yap, suggesting a convergence of Notch and Hippo in the endocardium at the level of Yap nuclear translocation. Genetic ablation of *Yap* or *Notch1/Rbpj* in the presumptive valve endocardium impairs valve formation through downregulation of the endocardial-to-mesenchymal transition driver *Snai1* resulting in hypocellular endocardial cushions.[48,63] However, while endothelial *Yap* deletion reduces endocardial proliferation,[63] Notch signaling ablation leads to a hyperproliferative endocardium.[64] This suggests that the Yap chromatin targets

promoting endocardial proliferation may become active after Notch inactivation. Endothelial ablation of the tumor suppressor Vgll4, a Yap competitor to bind Tead, results in the upregulation of Yap targets, valve mesenchyme hyperproliferation, and valve malformation,[65] a phenotype similar to that of *Jag1* inactivation.[7] While Notch and Vgll4 cooperation has been reported in erythropoiesis,[66] their potential cooperation in the endocardium has not been explored. Several studies have investigated the crosstalk between Notch and Hippo, revealing direct cooperative interaction in various contexts, such as Yap-Tead forming a transcriptional complex with the Notch target Hes1,[67] Yap/Taz directly interacting with NICD in a Tead-independent manner,[68] or NICD and Yap independently binding to the same enhancer.[69] Additionally, both positive crosstalk[70,71] and Notch inhibition by Yap have been reported.[72] Further research is required to elucidate the underlying mechanisms of the functional relationship between Notch and Yap in the embryonic endocardium and its implications for cardiac development and disease.

ARTICLE INFORMATION

Received August 2, 2023; revision received October 26, 2023; accepted October 31, 2023.

Affiliations

Intercellular Signaling in Cardiovascular Development and Disease Laboratory, Centro Nacional de Investigaciones Cardiovasculares Carlos III (CNIC), Madrid, Spain (L.L.-Z., B.G.F.-G., D.G., M.S.-A., J.L.d.l.P.). Ciber CV, Madrid, Spain (L.L.-Z., B.G.F.-G., D.G., M.S.-A., J.L.d.l.P.). Developmental Biology, Centre for Clinical, Experimental Surgery and Translational Research, Biomedical Research Foundation Academy of Athens, Greece (D.G.).

Acknowledgments

We thank E. Diaz for zebrafish husbandry and A. Galicia and L. Méndez for mouse husbandry; the CNIC (Centro Nacional de Investigaciones Cardiovasculares Carlos III) Flow Cytometry Unit for Fluorescence-activated cell sorting (FACS); the CNIC Genomics Unit for RNA-seq; Centro Nacional de Análisis Genómico (CNAG-CRG) for high throughput sequencing for ATAC-seq (assay for transposase-accessible chromatin with sequencing); the CNIC Bioinformatics Unit for RNA-seq and ATAC-seq data analysis; P.A. M. Jaramillo, S. Urra, and D. Muñoz for experimental work; and S. Bartlett for English editing.

Sources of Funding

This study was supported by grants PID2019-104776RB-I00, CB16/11/00399 (CIBER CV) from Ministerio de Ciencia e Innovación (MCIN)/Agencia Española de Investigación (AEI)/10.13039/501100011033, a grant from the Fundación BBVA (Ref.: BIO14_298), a grant from Fundació La Marató de TV3 (Ref.: 20153431), and a grant from the Spanish Society for Cardiology (SECSCFG-INV-CFG 21/004) to J.L. de la Pompa; and grants PID2019-110155RA-I00 and AC18/00047 to L. Luna-Zurita. The Ramón y Cajal postdoctoral contract (RYC-2016 to 20917) founded L. Luna-Zurita and supported the study. The cost of this publication was supported in part with funds from the European Regional Development Fund. The Centro Nacional de Investigaciones Cardiovasculares Carlos III (CNIC) is supported by the ISCIII, the MCIN, and the Pro CNIC Foundation and is a Severo Ochoa Center of Excellence (grant CEX2020001041-S) financed by MCIN/AEI/10.13039/501100011033.

Disclosures

None.

Supplemental Material

Expanded Materials and Methods
Figures S1–S5
Tables S1–S7
Major Resources Table
References 73–96

REFERENCES

1. Harris IS, Black BL. Development of the endocardium. *Pediatr Cardiol*. 2010;31:391–399. doi: 10.1007/s00246-010-9642-8
2. Zhang H, Lui KO, Zhou B. Endocardial cell plasticity in cardiac development, diseases and regeneration. *Circ Res*. 2018;122:774–789. doi: 10.1161/CIRCRESAHA.117.312136
3. MacGrogan D, Münch J, de la Pompa JL. Notch and interacting signalling pathways in cardiac development, disease, and regeneration. *Nat Rev Cardiol*. 2018;15:685–704. doi: 10.1038/s41569-018-0100-2
4. Mumm JS, Schroeter EH, Saxena MT, Griesemer A, Tian X, Pan DJ, Ray WJ, Kopan R. A ligand-induced extracellular cleavage regulates γ-secretase-like proteolytic activation of Notch1. *Mol Cell*. 2000;5:197–206. doi: 10.1016/s1097-2765(00)80416-5
5. Kopan R, Ilagan MXG. The canonical Notch signaling pathway: unfolding the activation mechanism. *Cell*. 2009;137:216–233. doi: 10.1016/j.cell.2009.03.045
6. Wang Y, Fang Y, Lu P, Wu B, Zhou B. NOTCH signaling in aortic valve development and calcific aortic valve disease. *Front Cardiovasc Med*. 2021;8:682298. doi: 10.3389/fcvm.2021.682298
7. MacGrogan D, D'Amato G, Travisano S, Martinez-Poveda B, Luxan G, Del Monte-Nieto G, Papoutsi T, Sbroggio M, Bou V, Gomez-Del Arco P, et al. Sequential ligand-dependent Notch signaling activation regulates valve primordium formation and morphogenesis. *Circ Res*. 2016;118:1480–1497. doi: 10.1161/CIRCRESAHA.115.308077
8. Li L, Krantz ID, Deng Y, Genin A, Banta AB, Collins CC, Qi M, Trask BJ, Kuo WL, Cochran J, et al. Alagille syndrome is caused by mutations in human Jagged1, which encodes a ligand for notch1. *Nat Genet*. 1997;16:243–251. doi: 10.1038/ng0797-243
9. Oda T, Elkahloun AG, Pike BL, Okajima K, Krantz ID, Genin A, Piccoli DA, Meltzer PS, Spinner NB, Collins FS, et al. Mutations in the human Jagged1 gene are responsible for Alagille syndrome. *Nat Genet*. 1997;16:235–242. doi: 10.1038/ng0797-235
10. Garg V, Muth AN, Ransom JF, Schluterman MK, Barnes R, King IN, Grossfeld PD, Srivastava D. Mutations in NOTCH1 cause aortic valve disease. *Nature*. 2005;437:270–274. doi: 10.1038/nature03940
11. Siguero-Álvarez M, Salguero-Jiménez A, Grego-Bessa J, De La Barrera J, Macgrogan D, Prados B, Sánchez-Sáez F, Piñeiro-Sabarís R, Felipe-Medina N, Torroja C, et al. A human hereditary cardiomyopathy shares a genetic substrate with bicuspid aortic valve. *Circulation*. 2023;147:47–65. doi: 10.1161/CIRCULATIONAHA.121.058767
12. Yang B, Zhou W, Jiao J, Nielsen JB, Mathis MR, Heydarpour M, Lettre G, Folkersen L, Prakash S, Schurmann C, et al. Protein-altering and regulatory genetic variants near GATA4 implicated in bicuspid aortic valve. *Nat Commun*. 2017;8:15481. doi: 10.1038/ncomms15481
13. Helgadottir A, Thorleifsson G, Gretarsdottir S, Stefansson OA, Tragante V, Thorolfsdottir RB, Jonsdottir I, Bjornsson T, Steinthorsdottir V, Verweij N, et al. Genome-wide analysis yields new loci associating with aortic valve stenosis. *Nat Commun*. 2018;9:987. doi: 10.1038/s41467-018-03252-6
14. Kyryachenko S, Georges A, Yu M, Barrandou T, Guo L, Bruneval P, Rubio T, Gronwald J, Baraki H, Kutschka I, et al. Chromatin accessibility of human mitral valves and functional assessment of MVP risk loci. *Circ Res*. 2021;128:e84–e101. doi: 10.1161/CIRCRESAHA.120.317581
15. D'Amato G, Luxan G, del Monte-Nieto G, Martinez-Poveda B, Torroja C, Walter W, Bochter MS, Benedito R, Cole S, Martinez F, et al. Sequential Notch activation regulates ventricular chamber development. *Nat Cell Biol*. 2016;18:7–20. doi: 10.1038/ncb3280
16. Torregrosa-Carrión R, Luna-Zurita L, García-Marqués F, D'Amato G, Piñeiro-Sabarís R, Bonzón-Kulichenko E, Vázquez J, de la Pompa JL. NOTCH activation promotes valve formation by regulating the endocardial secretome. *MolCellProteomics*.2019;18:1782–1795.doi:10.1074/mcp.RA119.001492
17. Benedito R, Roca C, Sorensen I, Adams S, Gossler A, Fruttiger M, Adams RH. The notch ligands Dll4 and Jagged1 have opposing effects on angiogenesis. *Cell*. 2009;137:1124–1135. doi: 10.1016/j.cell.2009.03.025
18. Manderfield LJ, High FA, Engleka KA, Liu F, Li L, Rentschler S, Epstein JA. Notch activation of Jagged1 contributes to the assembly of the arterial wall. *Circulation*. 2012;125:314–323. doi: 10.1161/CIRCULATIONAHA.111.047159
19. Palmer WH, Jia D, Deng WM. Cis-interactions between Notch and its ligands block ligand-independent Notch activity. *Elife*. 2014;3:e04415. doi: 10.7554/eLife.04415
20. Nandagopal N, Santat LA, Elowitz MB. Cis-activation in the Notch signaling pathway. *Elife*. 2019;8:e37880. doi: 10.7554/eLife.37880
21. Xu X, Seymour PA, Sneppen K, Trusina A, Egeskov-Madsen AR, Jørgensen MC, Jensen MH, Serup P. Jag1-Notch cis-interaction determines

cell fate segregation in pancreatic development. *Nat Commun*. 2023;14:348. doi: 10.1038/s41467-023-35963-w
22. MacGrogan D, Martínez-Poveda B, Desvignes J-P, Fernandez-Friera L, Gomez MJ, Gil Vilariño E, Callejas Alejano S, Garcia-Pavia P, Solis J, Lucena J, et al. Identification of a peripheral blood gene signature predicting aortic valve calcification. *Physiol Genomics*. 2020;52:563–574. doi: 10.1152/physiolgenomics.00034.2020
23. del Monte-Nieto G, Ramialison M, Adam AAS, Wu B, Aharonov A, D'uva G, Bourke LM, Pitulescu ME, Chen H, de la Pompa JL, et al. Control of cardiac jelly dynamics by NOTCH1 and NRG1 defines the building plan for trabeculation. *Nature*. 2018;557:439–445. doi: 10.1038/s41586-018-0110-6
24. Poulsen LC, Edelmann RJ, Krüger S, Diéguez-Hurtado R, Shah A, Stav-Noraas TE, Renzi A, Szymanska M, Wang J, Ehling M, et al. Inhibition of endothelial NOTCH1 signaling attenuates inflammation by reducing cytokine-mediated histone acetylation at inflammatory enhancers. *Arterioscler Thromb Vasc Biol*. 2018;38:854–869. doi: 10.1161/ATVBAHA.117.310388
25. Morikawa M, Koinuma D, Tsutsumi S, Vasilaki E, Kanki Y, Heldin C-H, Aburatani H, Miyazono K. ChIP-seq reveals cell type-specific binding patterns of BMP-specific Smads and a novel binding motif. *Nucleic Acids Res*. 2011;39:8712–8727. doi: 10.1093/nar/gkr572
26. Ramachandran A, Vizán P, Das D, Chakravarty P, Vogt J, Rogers KW, Müller P, Hinck AP, Sapkota GP, Hill CS. TGF-β uses a novel mode of receptor activation to phosphorylate SMAD1/5 and induce epithelial-to-mesenchymal transition. *Elife*. 2018;7:e31756. doi: 10.7554/eLife.31756
27. Papoutsi T, Luna-Zurita L, Prados B, Zaffran S, de la Pompa JL. Bmp2 and Notch cooperate to pattern the embryonic endocardium. *Development*. 2018;145:dev163378. doi: 10.1242/dev.163378
28. Horisawa K, Udono M, Ueno K, Ohkawa Y, Nagasaki M, Sekiya S, Suzuki A. The dynamics of transcriptional activation by hepatic reprogramming factors. *Mol Cell*. 2020;79:660–676.e8. doi: 10.1016/j.molcel.2020.07.012
29. Hass MR, Brissette D, Parameswaran S, Pujato M, Donmez O, Kottyan LC, Weirauch MT, Kopan R. Runx1 shapes the chromatin landscape via a cascade of direct and indirect targets. *PLoS Genet*. 2021;17:e1009574. doi: 10.1371/journal.pgen.1009574
30. Kathiriya IS, King IN, Murakami M, Nakagawa M, Astle JM, Gardner KA, Gerard RD, Olson EN, Srivastava D, Nakagawa O. Hairy-related transcription factors inhibit GATA-dependent cardiac gene expression through a signal-responsive mechanism. *J Biol Chem*. 2004;279:54937–54943. doi: 10.1074/jbc.M409879200
31. Fischer A, Klattig J, Kneitz B, Diez H, Maier M, Holtmann B, Englert C, Gessler M. Hey basic Helix-Loop-Helix transcription factors are repressors of GATA4 and GATA6 and restrict expression of the GATA target gene ANF in fetal hearts. *Mol Cell Biol*. 2005;25:8960–8970. doi: 10.1128/MCB.25.20.8960-8970.2005
32. Zhou P, Zhang Y, Sethi I, Ye L, Trembley MA, Cao Y, Akerberg BN, Xiao F, Zhang X, Li K, et al. GATA4 regulates developing endocardium through interaction with ETS1. *Circ Res*. 2022;131:e152–e168. doi: 10.1161/CIRCRESAHA.120.318102
33. Li R-G, Xu Y-J, Wang J, Liu X-Y, Yuan F, Huang R-T, Xue S, Li L, Liu H, Li Y-J, et al. GATA4 loss-of-function mutation and the congenitally bicuspid aortic valve. *Am J Cardiol*. 2018;121:469–474. doi: 10.1016/j.amjcard.2017.11.012
34. Gharibeh L, Komati H, Bossé Y, Boodhwani M, Heydarpour M, Fortier M, Hassanzadeh R, Ngu J, Mathieu P, Body S, et al; Bicuspid Aortic Valve Consortium. GATA6 regulates aortic valve remodeling, and its haploinsufficiency leads to right-left type bicuspid aortic valve. *Circulation*. 2018;138:1025–1038. doi: 10.1161/CIRCULATIONAHA.117.029506
35. Goode DK, Obier N, Vijayabaskar MS, Lie-A-Ling M, Lilly AJ, Hannah R, Lichtinger M, Batta K, Florkowska M, Patel R, et al. Dynamic gene regulatory networks drive hematopoietic specification and differentiation. *Dev Cell*. 2016;36:572–587. doi: 10.1016/j.devcel.2016.01.024
36. Akerberg BN, Gu F, VanDusen NJ, Zhang X, Dong R, Li K, Zhang B, Zhou B, Sethi I, Ma Q, et al. A reference map of murine cardiac transcription factor chromatin occupancy identifies dynamic and conserved enhancers. *Nat Commun*. 2019;10:4907. doi: 10.1038/s41467-019-12812-3
37. Lambertini C, Pantano S, Dotto GP. Differential control of Notch1 gene transcription by Klf4 and Sp3 transcription factors in normal versus cancer-derived keratinocytes. *PLoS One*. 2010;5:e10369. doi: 10.1371/journal.pone.0010369
38. Hale AT, Tian H, Anih E, Recio FO, Shatat MA, Johnson T, Liao X, Ramirez-Bergeron DL, Proweller A, Ishikawa M, et al. Endothelial Kruppel-like factor 4 regulates angiogenesis and the Notch signaling pathway. *J Biol Chem*. 2014;289:12016–12028. doi: 10.1074/jbc.M113.530956
39. Boogerd CJ, Aneas I, Sakabe N, Dirschinger RJ, Cheng QJ, Zhou B, Chen J, Nobrega MA, Evans SM. Probing chromatin landscape reveals roles of endocardial TBX20 in septation. *J Clin Invest*. 2016;126:3023–3035. doi: 10.1172/JCI85350
40. Fishman MC. gridlock, an HLH gene required for assembly of the aorta in zebrafish. *Science*. 2000;287:1820–1824. doi: 10.1126/science.287.5459.1820
41. Zhong TP, Childs S, Leu JP, Fishman MC. Gridlock signalling pathway fashions the first embryonic artery. *Nature*. 2001;414:216–220. doi: 10.1038/35102599
42. Gibb N, Lazic S, Yuan X, Deshwar AR, Leslie M, Wilson MD, Scott IC. Hey2 regulates the size of the cardiac progenitor pool during vertebrate heart development. *Development*. 2018;145:dev167510. doi: 10.1242/dev.167510
43. Liu Y, Wang G, Yang Y, Mei Z, Liang Z, Cui A, Wu T, Liu C-Y, Cui L. Increased TEAD4 expression and nuclear localization in colorectal cancer promote epithelial-mesenchymal transition and metastasis in a YAP-independent manner. *Oncogene*. 2016;35:2789–2800. doi: 10.1038/onc.2015.342
44. Park B, Chang S, Lee G-J, Kang B, Kim JK, Park H. Wnt3a disrupts GR-TEAD4-PPARγ2 positive circuits and cytoskeletal rearrangement in a β-catenin-dependent manner during early adipogenesis. *Cell Death Dis*. 2019;10:16. doi: 10.1038/s41419-018-1249-7
45. He L, Yuan L, Sun Y, Wang P, Zhang H, Feng X, Wang Z, Zhang W, Yang C, Zeng YA, et al. Glucocorticoid receptor signaling activates TEAD4 to promote breast cancer progression. *Cancer Res*. 2019;79:4399–4411. doi: 10.1158/0008-5472.CAN-19-0012
46. Monroe TO, Hill MC, Morikawa Y, Leach JP, Heallen T, Cao S, Krijger PHL, de Laat W, Wehrens XHT, Rodney GG, et al. YAP partially reprograms chromatin accessibility to directly induce adult cardiogenesis in vivo. *Dev Cell*. 2019;48:765–779.e7. doi: 10.1016/j.devcel.2019.01.017
47. Ong YT, Andrade J, Armbruster M, Shi C, Castro M, Costa ASH, Sugino T, Eelen G, Zimmermann B, Wilhelm K, et al. A YAP/TAZ-TEAD signalling module links endothelial nutrient acquisition to angiogenic growth. *Nat Metab*. 2022;4:672–682. doi: 10.1038/s42255-022-00584-y
48. Timmerman LA, Grego-Bessa J, Raya A, Bertran E, Perez-Pomares JM, Diez J, Aranda S, Palomo S, McCormick F, Izpisúa-Belmonte JC, et al. Notch promotes epithelial-mesenchymal transition during cardiac development and oncogenic transformation. *Genes Dev*. 2004;18:99–115. doi: 10.1101/gad.276304
49. Ma L, Lu MF, Schwartz RJ, Martin JF. Bmp2 is essential for cardiac cushion epithelial-mesenchymal transition and myocardial patterning. *Development*. 2005;132:5601–5611. doi: 10.1242/dev.02156
50. Xie X, Kaoud TS, Edupuganti R, Zhang T, Kogawa T, Zhao Y, Chauhan GB, Giannoukos DN, Qi Y, Tripathy D, et al. C-Jun N-terminal kinase promotes stem cell phenotype in triple-negative breast cancer through upregulation of Notch1 via activation of c-Jun. *Oncogene*. 2017;36:2599–2608. doi: 10.1038/onc.2016.417
51. Forghany Z, Robertson F, Lundby A, Olsen JV, Baker DA. Control of endothelial cell tube formation by Notch ligand intracellular domain interactions with activator protein 1 (AP-1). *J Biol Chem*. 2018;293:1229–1242. doi: 10.1074/jbc.M117.819045
52. Seo S, Kume T. Forkhead transcription factors, Foxc1 and Foxc2, are required for the morphogenesis of the cardiac outflow tract. *Dev Biol*. 2006;296:421–436. doi: 10.1016/j.ydbio.2006.06.012
53. Mohamed SA, Aherrahrou Z, Liptau H, Erasmi AW, Hagemann C, Wrobel S, Borzym K, Schunkert H, Sievers HH, Erdmann J. Novel missense mutations (pT596M and pP1797H) in NOTCH1 in patients with bicuspid aortic valve. *Biochem Biophys Res Commun*. 2006;345:1460–1465. doi: 10.1016/j.bbrc.2006.05.046
54. McKellar SH, Tester DJ, Yagubyan M, Majumdar R, Ackerman MJ, Sundt TM. Novel NOTCH1 mutations in patients with bicuspid aortic valve disease and thoracic aortic aneurysms. *J Thorac Cardiovasc Surg*. 2007;134:290–296. doi: 10.1016/j.jtcvs.2007.02.041
55. Burns CE, Traver D, Mayhall E, Shepard JL, Zon LI. Hematopoietic stem cell fate is established by the Notch-Runx pathway. *Genes Dev*. 2005;19:2331–2342. doi: 10.1101/gad.1337005
56. Rodríguez-Caparrós A, García V, Casal A, López-Ros J, García-Mariscal A, Tani-ichi S, Ikuta K, Hernández-Munain C. Notch signaling controls transcription via the recruitment of RUNX1 and MYB to enhancers during T cell development. *J Immunol*. 2019;202:2460–2472. doi: 10.4049/jimmunol.1801650
57. Tang CY, Wu M, Zhao D, Edwards D, McVicar A, Luo Y, Zhu G, Wang Y, Zhou H-D, Chen W, et al. Runx1 is a central regulator of osteogenesis for bone homeostasis by orchestrating BMP and WNT signaling pathways. *PLoS Genet*. 2021;17:e1009233. doi: 10.1371/journal.pgen.1009233
58. Theodoris CV, Li M, White MP, Liu L, He D, Pollard KS, Bruneau BG, Srivastava D. Human disease modeling reveals integrated transcriptional and epigenetic

mechanisms of NOTCH1 haploinsufficiency. *Cell*. 2015;160:1072–1086. doi: 10.1016/j.cell.2015.02.035
59. Currey L, Thor S, Piper M. TEAD family transcription factors in development and disease. *Development*. 2021;148:dev196675. doi: 10.1242/dev.196675
60. Xin M, Kim Y, Sutherland LB, Qi X, McAnally J, Schwartz RJ, Richardson JA, Bassel-Duby R, Olson EN. Regulation of insulin-like growth factor signaling by Yap governs cardiomyocyte proliferation and embryonic heart size. *Sci Signal*. 2011;4:ra70. doi: 10.1126/scisignal.2002278
61. Gründl M, Walz S, Hauf L, Schwab M, Werner KM, Spahr S, Schulte C, Maric HM, Ade CP, Gaubatz S. Interaction of YAP with the Myb-MuvB (MMB) complex defines a transcriptional program to promote the proliferation of cardiomyocytes. *PLoS Genet*. 2020;16:e1008818. doi: 10.1371/journal.pgen.1008818
62. Aharonov A, Shakked A, Umansky KB, Savidor A, Genzelinakh A, Kain D, Lendengolts D, Revach O-Y, Morikawa Y, Dong J, et al. ERBB2 drives YAP activation and EMT-like processes during cardiac regeneration. *Nat Cell Biol*. 2020;22:1346–1356. doi: 10.1038/s41556-020-00588-4
63. Zhang H, Von Gise A, Liu Q, Hu T, Tian X, He L, Pu W, Huang X, He L, Cai C-L, et al. Yap1 Is required for endothelial to mesenchymal transition of the atrioventricular cushion. *J Biol Chem*. 2014;289:18681–18692. doi: 10.1074/jbc.M114.554584
64. Grego-Bessa J, Luna-Zurita L, del Monte G, Bolos V, Melgar P, Arandilla A, Garratt AN, Zang H, Mukouyama Y-S, Chen H, et al. Notch signaling is essential for ventricular chamber development. *Dev Cell*. 2007;12:415–429. doi: 10.1016/j.devcel.2006.12.011
65. Yu W, Ma X, Xu J, Heumüller AW, Fei Z, Feng X, Wang X, Liu K, Li J, Cui G, et al. VGLL4 plays a critical role in heart valve development and homeostasis. *PLoS Genet*. 2019;15:e1007977. doi: 10.1371/journal.pgen.1007977
66. Wang Y, Liu X, Xie B, Yuan H, Zhang Y, Zhu J. The NOTCH1-dependent HIF1α/VGLL4/IRF2BP2 oxygen sensing pathway triggers erythropoiesis terminal differentiation. *Redox Biol*. 2020;28:101313. doi: 10.1016/j.redox.2019.101313
67. Cebola I, Rodríguez-Seguí SA, Cho CH-H, Bessa J, Rovira M, Luengo M, Chhatriwala M, Berry A, Ponsa-Cobas J, Maestro MA, et al. TEAD and YAP regulate the enhancer network of human embryonic pancreatic progenitors. *Nat Cell Biol*. 2015;17:615–626. doi: 10.1038/ncb3160
68. Manderfield LJ, Aghajanian H, Engleka KA, Lim LY, Liu F, Jain R, Li L, Olson EN, Epstein JA. Hippo signaling is required for Notch-dependent smooth muscle differentiation of neural crest. *Development*. 2015;142:2962–2971. doi: 10.1242/dev.125807
69. Rayon T, Menchero S, Nieto A, Xenopoulos P, Crespo M, Cockburn K, Cañon S, Sasaki H, Hadjantonakis A-K, de la Pompa JL, et al. Notch and hippo converge on Cdx2 to specify the trophectoderm lineage in the mouse blastocyst. *Dev Cell*. 2014;30:410–422. doi: 10.1016/j.devcel.2014.06.019
70. Wu N, Nguyen Q, Wan Y, Zhou T, Venter J, Frampton GA, DeMorrow S, Pan D, Meng F, Glaser S, et al. The Hippo signaling functions through the Notch signaling to regulate intrahepatic bile duct development in mammals. *Lab Invest*. 2017;97:843–853. doi: 10.1038/labinvest.2017.29
71. Li Y, Hibbs MA, Gard AL, Shylo NA, Yun K. Genome-wide analysis of N1ICD/RBPJ targets in vivo reveals direct transcriptional regulation of Wnt, SHH, and hippo pathway effectors by Notch1. *Stem Cells*. 2012;30:741–752. doi: 10.1002/stem.1030
72. Yasuda D, Kobayashi D, Akahoshi N, Ohto-Nakanishi T, Yoshioka K, Takuwa Y, Mizuno S, Takahashi S, Ishii S. Lysophosphatidic acid-induced YAP/TAZ activation promotes developmental angiogenesis by repressing Notch ligand Dll4. *J Clin Invest*. 2019;129:4332–4349. doi: 10.1172/JCI121955
73. Grivas D, González-Rajal A, Guerrero Rodríguez C, Garcia R, de la Pompa JL. Loss of Caveolin-1 and caveolae leads to increased cardiac cell stiffness and functional decline of the adult zebrafish heart. *Sci Reports*. 2020;10:1–14. doi: 10.1038/s41598-020-68802-9
74. Grivas D, González-Rajal A, de la Pompa JL. Midkine-a regulates the formation of a fibrotic scar during zebrafish heart regeneration. *Front Cell Dev Biol*. 2021;9:1084. doi: 10.3389/FCELL.2021.669439
75. Cong L, Ran FA, Cox D, Lin S, Barretto R, Habib N, Hsu PD, Wu X, Jiang W, Marraffini LA, et al. Multiplex genome engineering using CRISPR/Cas systems. *Science (New York, N.Y.)*. 2013;339:819–823. doi: 10.1126/science.1231143
76. Lawson ND, Weinstein BM. In vivo imaging of embryonic vascular development using transgenic zebrafish. *Dev Biol*. 2002;248:307–318. doi: 10.1006/dbio.2002.0711
77. López-Guerra M, Xargay-Torrent S, Fuentes P, Roldán J, González-Farré B, Rosich L, Silkenstedt E, García-León MJ, Lee-Vergés E, Giménez N, et al. Specific NOTCH1 antibody targets DLL4-induced proliferation, migration, and angiogenesis in NOTCH1-mutated CLL cells. *Oncogene*. 2020;39:1185–1197. doi: 10.1038/s41388-019-1053-6
78. Martin M. Cutadapt removes adapter sequences from high-throughput sequencing reads. *EMBnetJournal*. 2011;17:10–12. doi: 10.14806/ej.17.1.200
79. Li B, Dewey CN. RSEM: accurate transcript quantification from RNA-Seq data with or without a reference genome. *BMC Bioinf*. 2011;12:323. doi: 10.1186/1471-2105-12-323
80. Metsalu T, Vilo J. ClustVis: a web tool for visualizing clustering of multivariate data using Principal Component Analysis and heatmap. *Nucleic Acids Res*. 2015;43:W566–W570. doi: 10.1093/nar/gkv468
81. Zhou Y, Zhou B, Pache L, Chang M, Khodabakhshi AH, Tanaseichuk O, Benner C, Chanda SK. Metascape provides a biologist-oriented resource for the analysis of systems-level datasets. *Nat Commun*. 2019;10:1–10. doi: 10.1038/s41467-019-09234-6
82. Mootha VK, Lindgren CM, Eriksson KF, Subramanian A, Sihag S, Lehar J, Puigserver P, Carlsson E, Ridderstråle M, Laurila E, et al. PGC-1α-responsive genes involved in oxidative phosphorylation are coordinately downregulated in human diabetes. *Nat Genet*. 2003;34:267–273. doi: 10.1038/ng1180
83. Subramanian A, Tamayo P, Mootha VK, Mukherjee S, Ebert BL, Gillette MA, Paulovich A, Pomeroy SL, Golub TR, Lander ES, et al. Gene set enrichment analysis: a knowledge-based approach for interpreting genome-wide expression profiles. *Proc Natl Acad Sci U S A*. 2005;102:15545–15550. doi: 10.1073/pnas.0506580102
84. Piñero J, Ramírez-Anguita JM, Saüch-Pitarch J, Ronzano F, Centeno E, Sanz F, Furlong LI. The DisGeNET knowledge platform for disease genomics: 2019 update. *Nucleic Acids Res*. 2020;48:D845–D855. doi: 10.1093/nar/gkz1021
85. Szklarczyk D, Gable AL, Nastou KC, Lyon D, Kirsch R, Pyysalo S, Doncheva NT, Legeay M, Fang T, Bork P, et al. The STRING database in 2021: customizable protein-protein networks, and functional characterization of user-uploaded gene/measurement sets. *Nucleic Acids Res*. 2021;49:10800. doi: 10.1093/nar/gkab835
86. Shannon P, Markiel A, Ozier O, Baliga NS, Wang JT, Ramage D, Amin N, Schwikowski B, Ideker T. Cytoscape: a software environment for integrated models of biomolecular interaction networks. *Genome Res*. 2003;13:2498–2504. doi: 10.1101/gr.1239303
87. Lara-Astiaso D, Weiner A, Lorenzo-Vivas E, Zaretsky I, Jaitin DA, David E, Keren-Shaul H, Mildner A, Winter D, Jung S, et al. Immunogenetics Chromatin state dynamics during blood formation. *Science*. 2014;345:943–949. doi: 10.1126/science.1256271
88. Langmead B, Salzberg SL. Fast gapped-read alignment with Bowtie 2. *Nat Methods*. 2012;9:357–359. doi: 10.1038/nmeth.1923
89. Li H, Handsaker B, Wysoker A, Fennell T, Ruan J, Homer N, Marth G, Abecasis G, Durbin R; 1000 Genome Project Data Processing Subgroup. The sequence alignment/map format and SAMtools. *Bioinformatics*. 2009;25:2078–2079. doi: 10.1093/bioinformatics/btp352
90. Zhang Y, Liu T, Meyer CA, Eeckhoute J, Johnson DS, Bernstein BE, Nusbaum C, Myers RM, Brown M, Li W, et al. Model-based analysis of ChIP-Seq (MACS). *Genome Biol*. 2008;9:R137. doi: 10.1186/GB-2008-9-9-R137
91. Broom BM, Ryan MC, Stucky M, Wakefield C, Melott JM, Akbani R, Weinstein JN. Interactive Clustered Heat Map Builder: an easy web-based tool for creating sophisticated clustered heat maps. *F1000Research*. 2019;8:ISCB Comm J-1750. doi: 10.12688/F1000RESEARCH.20590.2
92. McLean CY, Bristor D, Hiller M, Clarke SL, Schaar BT, Lowe CB, Wenger AM, Bejerano G. GREAT improves functional interpretation of cis-regulatory regions. *Nat Biotechnol*. 2010;28:495–501. doi: 10.1038/nbt.1630
93. Hinrichs AS, Karolchik D, Baertsch R, Barber GP, Bejerano G, Clawson H, Diekhans M, Furey TS, Harte RA, Hsu F, et al. The UCSC Genome Browser Database: update 2006. *Nucleic Acids Res*. 2006;34:D590–D598. doi: 10.1093/nar/gkj144
94. Afgan E, Baker D, Batut B, van den Beek M, Bouvier D, Čech M, Chilton J, Clements D, Coraor N, Grüning BA, et al. The Galaxy platform for accessible, reproducible and collaborative biomedical analyses: 2018 update. *Nucleic Acids Res*. 2018;46:W537–W544. doi: 10.1093/nar/gky379
95. Heinz S, Benner C, Spann N, Bertolino E, Lin YC, Laslo P, Cheng JX, Murre C, Singh H, Glass CK. Simple combinations of lineage-determining transcription factors prime cis-regulatory elements required for macrophage and B cell identities. *Mol Cell*. 2010;38:576–589. doi: 10.1016/j.molcel.2010.05.004
96. Kanzler B, Kuschert SJ, Liu YH, Mallo M. Hoxa-2 restricts the chondrogenic domain and inhibits bone formation during development of the branchial area. *Development*. 1998;125:2587–2597. doi: 10.1242/dev.125.14.2587